



Università degli Studi di Padova

Dipartimento di Tecnica e Gestione dei Sistemi Industriali

Corso di Laurea Magistrale in Ingegneria Meccatronica

Tesi di Laurea Magistrale

Design of an Automatic Electric Vehicle Batteries Discharging Station

Relatore: Prof. Boschetti Giovanni

Correlatore: Prof. Choux Martin

Laureando: Carnelos Davide

Anno Accademico 2021-2022

Acknowledgements

Prima di cominciare la trattazione del mio elaborato, ci tengo a ringraziare tutte le persone che in questi anni mi sono state vicine, permettendomi di compiere con successo questo importante passo della mia vita.

In particolare, ringrazio il mio relatore, Professor Giovanni Boschetti, per il supporto datomi lungo il mio percorso di tesi, soprattutto nelle ultime fasi, supportandomi e sapendomi consigliare come esporre al meglio il lavoro che ho svolto.

Ci tengo inoltre a ringraziare il mio relatore Norvegese, Professor Martin Marie Hubert Choux, per la sua sincera disponibilità e per avermi accompagnato diligentemente in ogni fase del mio lavoro, ascoltando le mie idee e credendo nelle soluzioni che ho proposto.

Ringrazio i miei amici e compagni di università, con i quali ho condiviso questi anni, che mi hanno aiutato a superare le difficoltà e ad alleggerire le mie giornate, senza dei quali non sarebbe stato lo stesso.

Infine, ringrazio di cuore tutta la mia famiglia, in particolare mia Madre e mio Padre, per avermi permesso di perseguire questo percorso, per aver sempre creduto in me e per avermi ascoltato e compreso quando più ne avevo bisogno, dandomi i giusti consigli per superare ogni avversità.

Abstract

The worldwide spread of electric mobility will lead to problems, in the near future, that have never been experienced before. In particular, the enormous quantity of lithium batteries that are the basis of this revolution will have to be disposed of or recycled. It is therefore of primary importance to develop an appropriate technological process to face this challenge. The work exhibited in this thesis is part of LIBRES, a Norwegian project owned by the company "Norsk Hydro", with the goal of finding fully-automated solutions for complete Lithium-Ion batteries recycling. The case study is the design of an automatic discharging station for electric vehicle batteries, focused on the artificial vision system, a structured light camera capable of detecting the battery connectors and locating them in 3D space; and on the feed-back control of the discharge process, based on the acquisition performed by a thermal camera, which monitor the process. The proposed automatic system significantly increases performance compared to manual discharge, currently performed, and furthermore increases safety standards.

Contents

Acknowledgements	i
Abstract	ii
1 Introduction	1
1.1 Industrial Motivations	2
1.1.1 The LIBRES project	3
1.2 Project Main Objectives	4
2 Theory on EV battery packs discharge	6
2.1 State of the Art	6
2.2 EV batteries end of life	11
2.2.1 Battery recycling	13
2.3 Cognitive Robotics	15
3 Methods	17
3.1 Discharge Strategy	17
3.1.1 Trade-off Aspects	17
3.1.2 Technical Limits	19
3.2 YOLO	21
3.3 Training phase	23
3.3.1 Images acquisition	23
3.3.2 Image labeling	24
3.3.3 Neural network training	25
3.4 Detection phase	28
3.5 Batteries discharge	29
3.6 Discharge control	30
3.7 Thermal Imaging	32
3.7.1 Flat Field Correction	36
4 Experimental Setup	41
4.1 Vision system setup	41
4.1.1 Robotic arm	41
4.1.2 Motion track	43
4.1.3 Robot Operating System core	43
4.1.4 Zivid structured light camera	44
4.1.5 Battery pack	45

4.2	Battery discharge setup	45
4.2.1	Programmable electronic load & DC power supply	47
4.2.2	Low voltage battery pack & BMS	48
4.2.3	Thermal camera & mechanical support	48
4.2.4	Control unit & Operating logic	49
5	Results and Discussion	52
5.1	Vision system	52
5.1.1	Training phase	52
5.1.2	Detection phase	56
5.1.3	Pose estimation	60
5.2	Discharge control	62
5.2.1	Open loop control	63
5.2.2	Closed loop control with FFC correction	66
5.2.3	Results discussion	68
6	Conclusions	71
A	Discharge control Python scripts	73
A.1	main.py	73
A.2	functions.py	79
A.3	thermal_camera.py	83
A.4	import_clr.py	84
B	Vision system Python scripts	86
B.1	paths_maker.py	86
	Bibliography	89

Chapter 1

Introduction

The global hybrid and electric vehicle market has grown tremendously in recent years, setting new historic sales records every year. This trend is confirmed to be stable, and is driven by the growing awareness of the environmental issues that this and future generations will have to face.

Climate change is nowadays the main concern when it comes to environmental issues, and one of its main causes has been identified in global warming, caused by excessive human activity.

Since the 19th century, with the industrial revolution, human activities have in fact been the main factor at the origin of climate change, essentially attributable to the combustion of fossil fuels (such as coal, oil and gas) which produces heat-retaining gases, known as greenhouse gases.

Carbon dioxide (CO_2) is one of this gases, and it is currently the most impactful one. Any activity involving combustion produces carbon dioxide as waste, including traditional internal combustion engines.

Although in the last 30 years in many sectors (such as agriculture, industry and energy supply) there has been a reduction in CO_2 emissions, and average European emissions are decreasing, the transport sector instead presents an opposite trend, with an increase in CO_2 produced by 30 million tons from 1990 to today. Road transport is nowadays one of the main responsible in CO_2 production.

In such a scenario, a feasible solution is seen in electric and hybrid mobility, which drastically reduces the production of CO_2 associated with transport, to the point of completely canceling it in the case of 100% electric vehicles.

Under this pressure, the sale of "green" cars has been encouraged by governments around the world and recently, on June 8th 2022, the European parliament voted in favor of an effective EU ban on the sale of new petrol and diesel cars from 2035, upholding a key pillar of the European Union's plans to cut net planet-warming emissions 55% by 2030, from 1990 levels, going in the direction of a 100% reduction in CO_2 emissions from new cars by 2035, making it impossible to sell fossil fuel-powered vehicles in the EU from that date [17].

The sale of Plug-in Hybrid Electric Vehicles (PHEV) and Battery Electric Vehicles (BEV) around the world has undergone a huge increase in the last decade. Canalys, leading global technology market analyst company, estimates that more than 6.5 million vehicles were sold in 2021 [4], following an exponential growth (Figure 1.1) [15].

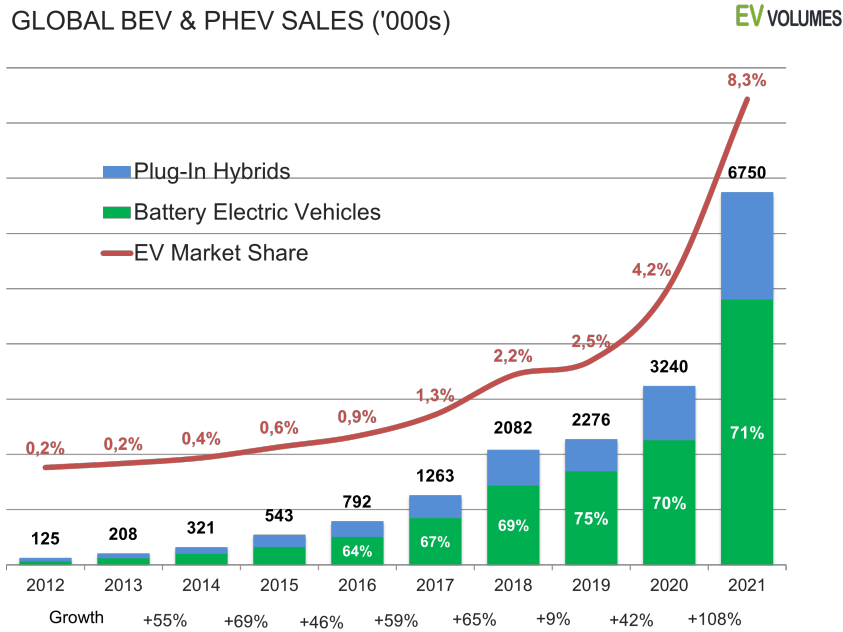


Figure 1.1: Worldwide sales of PHEV and BEV cars.

However, growing numbers of electric vehicles present a serious waste-management challenge for recycle at their end-of-life. With a life cycle around ten years, depending on the use, in the next decades there will be millions of batteries that will need to be managed.

Nowadays, battery recycling is mostly done manually, with consequent low efficiency and high times required for the process. Furthermore, traditional process presents a not negligible safety hazard due to the high-voltages involved when working with charged EV batteries. Scientific literature doesn't report any fully automated approach, and only few studies have been made in order to increase disassembly productivity thanks to human collaborative-robot cooperation [30].

With current sales volumes, the approach to recycling must also be updated, increasing productivity and efficiency, and creating plants capable of handling much higher numbers of batteries per unit of time.

In this project, automation is proposed as a solution, capable of dealing with high volumes, increasing productivity and safety for the human operators.

1.1 Industrial Motivations

Due to the constant growth in the number of electric vehicles, within a few decades an enormous number of lithium batteries, which have reached their end of life, will have to be recycled or disposed of. To manage this enormous quantity, it will be necessary to have a rapid, efficient, safe and sustainable technological process, capable of meeting the high request of work.

Nowadays, the process has not reached yet that degree of productivity. Electric battery packs are dismantled manually, the process requires two people, which must be authorised electricians with high voltage experience and it can take up to 45 minutes to manually disassemble a single pack [5].

The disassembly of lithium-ion battery systems from automotive applications is a complex

and therefore time and cost consuming process due to a wide variety of the battery designs, flexible components like cables, and potential dangers caused by high voltage and the chemicals contained in the battery cells. All these factors have to be considered when planning the disassembly processes and appropriate work stations [30].

This manual process is currently feasible due to the still relatively low volumes of work, however, with the inevitable growth that is expected, it will no longer be sustainable. For this reason, it is already necessary to move towards the direction of a more modern approach, able to handle higher quantities, in order to be prepared for future challenges.

The solution outlined in this report is part of a bigger project, which proposes automation as an answer to the problem. The aim is to develop a lithium-ion batteries recycling pilot plant in Norway, large enough to handle commercial volumes by 2024. The system is thought to have a high level of automation, integrating robotic arms, vision systems, artificial intelligence, automatic controls and autonomous decision making, accordingly with the paradigms of cognitive automation.

This approach will lead to a faster process, able to treat a greater number of batteries at the same time, reaching the required efficiency. Involving automation, the system is also more safe, not requiring direct contact between charged high voltage batteries and human operators, which in case of faults may turn fatal. Furthermore, the human error factor is eliminated, increasing the safety of the plant itself, which treats potentially incendiary or even explosive components (batteries).

1.1.1 The LIBRES project

LIBRES, that stands for Lithium-Ion Battery Recycling, is a Norwegian project which involves different national realities, including universities, companies and industrial partners, with the objective of developing a design basis for a lithium-ion battery recycling pilot plant in Norway, including automated disassembly of electric vehicle battery packs, modules and cells.

The research is funded by the "Research Council of Norway", government agency part of the Norwegian Ministry of Education and Research, starting in 2018 and until 2022. The head and main manager of the project is "Norsk Hydro ASA", leader company in aluminium and renewables industry, with years of experience in these fields. The company aims with this research to lay the foundation for a new, exciting industry related to the recycling of used electric car batteries in Norway. Country which has a unique position with the availability of these batteries, giving an excellent starting point [3].

University of Agder (UiA) is one of the research partners, mainly focused on battery dismantling automation process. The goal, is to create a system capable of dismantling and discharging electric batteries so that they can be reused or recycled (thus disposed of in order to extract the chemical components for reuse) [5].

Working on this field, an important collaborator, member of LIBRES too, is "BatteriRetur AS", the central electric vehicles battery waste handler in Norway, with years of experience in EV packs dismantling and disposal. The company is directly in contact with the university Faculty of Engineering, in order to give the practical information about how the process is currently carried out and how it can be improved. For this reason, the data they provided have been an important starting point for the development of this project.

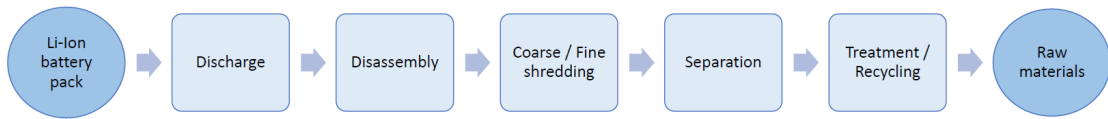


Figure 1.2: Recycle process phases for EV battery packs.

The work described in this document is one of the constituting projects of LIBRES.

1.2 Project Main Objectives

When battery packs reach their end of life there are 4 possible paths that can be taken:

- Re-use
- Recovery
- Recycling
- Disposal

The LIBRES project focuses on the recycling path, therefore on the the set of processes that, starting from the battery pack, lead to obtaining its raw components, which can be re-processed and used for other applications (e.g. battery cells or other electronic devices), following the paradigms of sustainable circular economy.

Recycling is divided into several phases, that follow a specific order, starting from discharge and gradually dismantling pack and modules, in order to obtain the single components that have to be treated for the purpose of extracting raw materials (figure 1.2).

LIBRES goal is to automate the full process, from the beginning to the end. With the aim of achieving this objective, firstly, single phases automation has to be designed, to be afterwards united into a unique industrial plant. In this thesis project, one part of the plant discussed above is treated, the discharge station.

Electrical discharge is the first step that has to be taken in place when dismantling a battery pack. For safety reasons, it is indeed necessary to reduce the potential danger that comes along with the high voltage (up to 400 V) of the batteries. After the discharge the batteries are disassembled before they are subject to a coarse shredding. Subsequently, the shredded material is separated of which one part is treated or recycled and the other part is subject to a fine crushing. After the fine crushing the materials are separated once more before they are also treated or recycled [30].

Battery discharge presents some complications and aspects that should not be overlooked in order to conduct a safe and effective process that doesn't cause any damage to the battery. The main risks associated with the discharge refer to the possibility of certain events occurring during the discharge:

- Risk of fire
- Risk of explosions

Both events may take place when the discharge is carried out too quickly, therefore with currents that exceed safety limits. This happens in the event of a short circuit, or in case of excessive discharge currents.

In such cases, high-currents may lead to heating and thermal runaway¹. Thermal runaway may result in the generation of particularly noxious byproducts, including hydrogen fluoride² (HF) gas, which along with other product gases may become trapped and ultimately result in cells exploding.

The cells also present a chemical hazard owing to the flammable electrolyte, toxic and carcinogenic electrolyte additives, and the potentially toxic or carcinogenic electrode materials [11].

Due to the presence of these risk factors, the optimal condition would result in conditions of:

- Absence of human operators
- Strict monitoring on the discharge process

In order to achieve this, a fully automated process results to be the best solution, for this reason, it is proposed an automatic discharge station as a solution.

The discharge process can be schematically divided into 3 phases, as reported in figure 1.3.

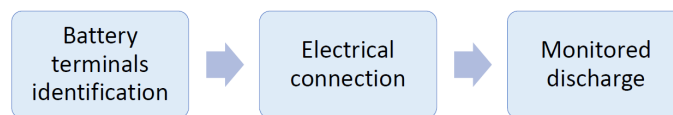


Figure 1.3: Automatic discharge station phases.

On this project, the first and the final phase of the discharge process, terminals identification and discharge monitoring, will be designed, implemented and tested, showing the improvements introduced by the proposed solutions.

In order to achieve this goal, two main sub-systems of the station will be involved:

- Computer vision system
- Control of the discharge

The design of these parts provides the training of a convolutional neural network, used to identify the terminals of the battery; their 3D-space position estimation, obtained starting from the location detected combined with the information from the structured light camera output point cloud; and finally the design of a discharge testing station, in order to test the discharge strategy to apply to the battery pack.

¹Thermal runaway describes a process that is accelerated by increased temperature, in turn releasing energy that further increases temperature. Thermal runaway occurs in situations where an increase in temperature changes the conditions in a way that causes a further increase in temperature, often leading to a destructive result. It is a kind of uncontrolled positive feedback. In chemistry and chemical engineering, thermal runaway is usually associated with strongly exothermic reactions that are accelerated by temperature rise, and this is the case of Lithium-Ion cells.

²Hydrogen fluoride is an extremely dangerous gas, forming corrosive and penetrating hydrofluoric acid upon contact with moisture. The gas can also cause blindness by rapid destruction of the corneas.

Chapter 2

Theory on EV battery packs discharge

There is no industry standard for discharging EV batteries. Many processes are suggested in literature with little information as to the methods used. A suitable process should be "safe", meaning it reduces the risk to the facility by minimizing the fire or explosion hazard and minimizes or eliminates human interaction with the battery pack. The process should also be "rapid", meaning it ensures that discharging does not become a bottleneck in recycling, "sustainable" meaning it has no polluting fluid waste streams and "feasible", then, mostly, cost efficient.

This chapter presents the main state of the art methods used in industrial EV discharge, and introduce an innovative approach to face this problem.

2.1 State of the Art

This project focuses on the discharge of batteries destined for recycling, this means that after discharge batteries are not meant anymore to be working, but they will be shredded and their materials recovered. Thinking about this perspective, the methodologies explained will consist in deep discharge, hence the process that bring the voltage level of single cells down to the lowest levels, close to 0 Volts.

The current industrial landscape presents mainly 3 possibilities to do deep discharge, that will be briefly explained below. Each one has pros and cons depending on the particular application considered, so it's not possible to identify one technique better than the others out of the application context [23].

Resistive Discharge

The resistive discharge with an electronic load method is the most conventional deep discharge method available in industry. The process simply consist on connecting the terminals of the battery to a resistive load (which can be variable) and let the current flow. Usually the battery energy is recovered and stored to be used for other scopes, or otherwise it can be converted in heat, for this reason it's important an appropriate cooling system integrated in the discharging station. The entire process has to be monitored, mainly being careful that temperature never go beyond safety limits. The resistance value is directly

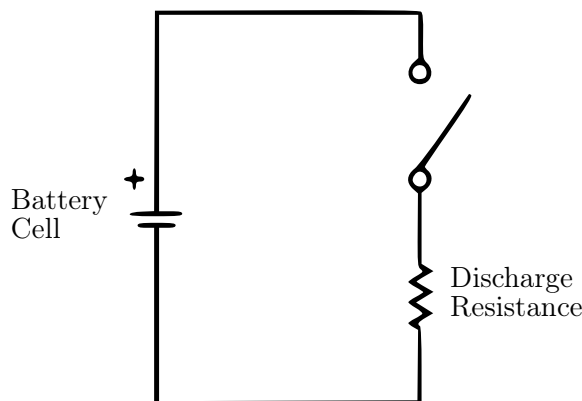


Figure 2.1: Discharge with resistive load schematics

related to the flowing current, so it's possible to act on this parameter to reduce the current intensity, with consequent reduction of the heat generated.

Compared to the other methods that will be explained, this technique offers many advantages, the main of which are: safety, in terms of fire and explosion hazard, which are minimized; rapidity, the discharge can be performed in a shorter time; sustainability, no chemical products involved and no pollution or refuse produced from the process and cost efficiency.

Furthermore, the possibility of monitor the battery parameters during the whole process, allows to perform the preferred discharge profile, that means that not only deep discharge can be realized, but it's also possible to discharge down to voltages level that doesn't break irreversibly the battery, allowing a second use.

On the other side, the main downside related to this approach, is the necessity of human interaction, to manually connect the discharge station to the battery terminals. When it comes to electric vehicle batteries, high voltages are involved, and so higher levels of human interaction are related with safety issues.

Salt Solution or Metal Powder

Deep discharge with salt solution is another method, more unconventional, that can be used in industry to discharge batteries. It consist on submerging a cell in a salt solution for a long time, up to 24 hours, recreating the conditions of a short circuit which slowly discharge the battery.

Going into more details, in this process, the dissolved salt acts as an electrolyte undergoing electrolysis, conducting electrons between the poles in a slow short circuit. This method has been discussed extensively in literature and has generally been accepted as viable. However, few sources cite the process in depth; discussing the mechanism or the state of the cell post submersion [24].

If the physical integrity is to be preserved, a more convenient setup consist on connect external wires to the poles of the battery and submerged them in aqueous salt solution, thus closing the circuit. The salt solution in this case acted as a controlled short circuit or as a primitive resistor, discharging the battery (see Figure 2.2 A). Using this setup, the battery was not placed in direct contact with the electrolyte solution and thus, its physical integrity is not compromised. With this approach, furthermore, it is possible to monitor the evolution of the electrical potential of the lithium-ion batteries, due only to

electro-chemical discharge (i.e., not attributable to physical damage to the battery).

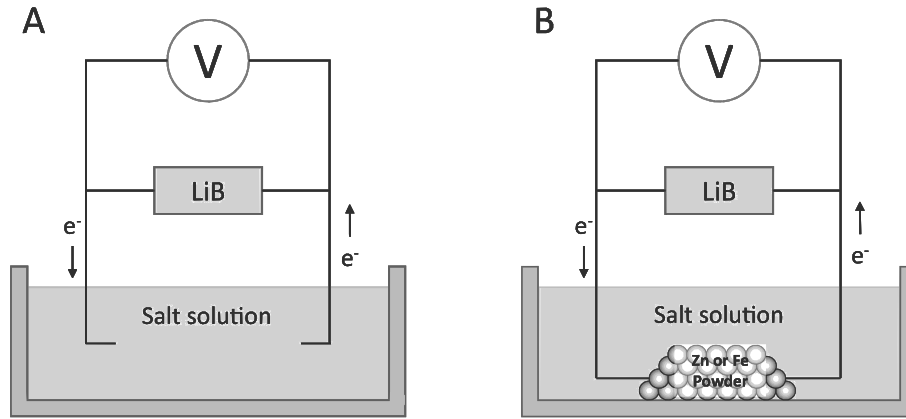


Figure 2.2: Discharge with salt solution and metal powder scheme

Compared to the resistive discharge, the main advantage given by this method is the minimization of the human interaction during the discharge process. No manual connection to the terminals is required, the batteries only need to be immersed in the solution to start the process. Fire and explosion hazard is usually low, preserving good safety standard as resistive discharge. Even with a view to automating the process, the saline solution allows interesting developments, because the entire battery pack can be immersed without having to disassemble it, but this kind of solution introduce new issues that will be discussed below.

Main disadvantages related to the use of salt solution are extreme slow time required to complete the deep discharge and the voltage rebound. Moreover, this solution is not as cost efficient as the first one, and it's less sustainable. The sustainability aspect might become even more critical when the whole battery pack is submerged, probable occurrence if you want to automate the process, as reported before. Corrosion of the cell casing causes leakage of the active materials and electrolyte, thereby releasing toxic substances or allowing self-ignition of the battery. Furthermore, submerging high voltage battery packs or modules in salt water can cause arcing and a resultant fire.

A more sophisticated approach, experimented by professor Severi Ojanen of Aalto University [24], has explored the concept of cathodic protection (see Figure 2.2 B). This process involves the addition of a more corrosion susceptible metallic element into the system. By doing so, the metallic element should preferentially corrode over the cell terminals or the platinum wire. In the set-up, the platinum wires to the cell were submerged in a salt solution and then connected to either side of the powder. The addition of this metallic element can drop the discharge time to a few minutes, and allows the batteries discharge to 0V.

A lesser known alternative is the method of placing the cells in a stainless-steel container with water and a metal powder. The water is meant to act as a buffer to thermal runaway while the metal acts as a conductive, low resistance path for short circuiting, which is an efficient method for ensuring the batteries are sufficiently deep discharged. The process, if not controlled, can artificially heat the battery, causing thermal runaway and self-ignition.

The risk of arcing in this method is greater than in the salt solution method since the conductivity of the metal is higher. If an entire EV pack is placed into the metal-water bath for discharging, there is the risk of high voltage arcing and significantly high temperature rise, potentially posing significant damage to the recycling facility.

Scientific literature report also similar experiment instead using graphite as a thermal buffer. However, the temperature of the cell increased rapidly, suggesting that graphite is not the most efficient thermal buffer in this procedure [10].

Inductive Discharge

Speaking of state-of-the-art technologies, in this section it was decided to report also inductive discharge, also known as wireless discharge, although it is a discharge technology mostly theorized rather than actually implemented in industrial practice. This method is suitable for future battery packs of all sizes equipped with wireless charging technology.

Inductive charging has gained notoriety of late, as phone and tablet companies attempt to find alternate ways for users to charge their devices, and automotive sector seems to be affected too by this trend. It can be conceived that future EV batteries would be equipped with a pad for wireless charging since there is an increasing demand for wireless technology (WiTricity). Therefore, the pads should be bidirectional so that all batteries entering the recycling facility can be discharged wirelessly. Since no physical connections to the batteries would be made, human contact with the battery would be nil. Additionally, the BMS could also be accessed wirelessly or by infrared. It should be equipped with an ‘override’ feature for recycling so that when the BMS is activated during discharging, it receives a signal indicating that it should allow for a discharge to 0V but still provide information on the SOH of the battery in terms of voltage, current and temperature. Honda and WiTricity have already proven that the discharged energy can be recovered in a vehicle to grid operation so, energy recovery would also be built into this model.

The concept of inductive discharging for batteries was born by the idea of having a wireless resistive discharge so that the manual component of connecting the batteries could be eliminated. Typically, only wireless charging is discussed in literature, however, the feasibility of bidirectional chargers has been explored by Honda and WiTricity. From their research, it is also possible to discharge a battery using this method in a vehicle-to-grid (V2G) operation [22].

The process of inductive charging is the similar to that of a transformer where a coil with a current passing through it, thereby creating a magnetic field, induces a current in another coil aligned with the magnetic field of the first. In the case of inductive charging, there is no metal connecting the coils to “allow” the transfer of the magnetic field, instead the two coils are magnetically coupled, through air, using an oscillator and a rectifier in resonance. Once the coils are in resonance, the current from the source is induced in the load and the device is charged. The shorter the distance between the two load and the source, the stronger the current.

However, for this method to work, a pad equipped with a coil and power electronics must be connected to the terminals of the battery. In order to avoid the manual step of connecting the pad to the terminals of the battery, this device should be installed in the battery by the manufacturer prior to installation in the vehicle. A receiving slab or pad must also be installed at the recycling facility. This receiver should be equipped with the secondary coil, power electronics and safety sensors so that the charging/discharging process does not destroy the battery and to protect the user since the magnetic field exposure is higher than is allowed by international regulations.

The system of discharging the battery would be equivalent to that of the resistive method, so the same procedure used for resistive discharge could be transferred to the inductive discharge method. However, currently, inductive charging pads are not regularly installed in mass distributed EVs, but it exist many real life implementations that shows how it is possible to use this technology, such as the Bombardier Primove e-buses, fully electric buses equipped with wireless charging, actually working in many cities in Germany, Belgium and Sweden [9]. In Primove project, the process inducts 200kW of power to an electric bus in approximately seven minutes.



Figure 2.3: Inductive discharge

Inert Crushing without Discharge

In battery recycling it's commonly used also a completely different approach than the other ones previously explained. It consists in avoiding the discharge process of the battery and shred them still charged. Shredding batteries which SOC level hasn't been take down to low levels is extremely dangerous, because of the related firing and explosion hazard, for this reason, it is necessary to adopt some precautions to avoid this and crush them safely. This process is called inert crushing.

Inert crushing usually includes dismantling the battery pack and then crush the modules or cells in an inert environment. The environment is made inert by a flow of gas such as carbon dioxide, nitrogen or argon, or cryogenically cooling the batteries prior to crushing. The inert gas method ensures that the cell is unable to ignite, even if there is a spark, due to the lack of oxygen in the atmosphere. Cryogenically freezing the cells reduces the reactivity of Lithium by 5 or 6 orders of magnitude, so that any exothermic reactions would occur so slowly that they would not be observed. Other methods include wet crushing with a solution that will not react with the electrolyte and will convert the Lithium to a nonreactive state or having a liquid spray in the presence of nitrogen while crushing.

On the other side, also thermal pre-treatment of the batteries has been explored. In this method the batteries are heated until the casing splits, the anode and cathode materials are deactivated and the electrolyte evaporates. Temperatures must arrive at 300°C either by solely heating or with the addition of pressure. By either mechanism the process is energy intensive and releases fine particulates. Thermal pre-treatment leads more serious environmental issues, that has to be properly handled.

The main downside of Inert Crushing methods is their cost. To give an example, ap-

proximately 1 kg of batteries can requires up to 2 hours of liquid nitrogen flow in order to arrive at cryogenic temperatures for crushing, with consequent costs. The flow of ‘inert’ gases for crushing require a precise control system, since the oxygen or moisture within the casing of the cells or modules could trigger a fire. Then, in wet crushing methods, a high volume of waste water must be treated post crushing, which is an energy intensive process.

Often in industry, deep discharging and inert crushing are typically coupled due to the high energy content of Electric Vehicle batteries. Even if the electrical hazard from the cells is minimized by deep discharging, the flammable components within the electrolyte could be ignited by even a small spark.

2.2 EV batteries end of life

The end of life (EOL) of a battery is the moment in which the battery is no longer suitable to operate in conditions close to the rated ones, for the application it has been designed for.

For EV batteries, a widely used retirement criterion was first introduced by the United States Advanced Battery Consortium (USABC) in 1996, which states that the battery pack should be replaced when it loses 20% of its original capacity. Therefore battery end-of-life is when 70–80% of original energy capacity remains, in other words a battery pack has to retire when its metric state-of-health (SOH) drops to 80% [28].

Serving on an electric vehicle is a tough environment for batteries, which typically undergo more than 1,000 charging/discharging incomplete cycles in 5–10 years and are subject to a wide temperatures range between 20°C and 70°C, high depth of discharge (DOD), and high rate charging and discharging (high power).

When an EV battery pack becomes unable to satisfy the use standard of EVs, it is usually removed from the car and replaced with a new battery, marking the end of its automotive life.

Making conservative assumptions, of an average battery pack weight of 250 kg and volume of half a cubic metre, 1 million of battery packs (which is approximately the number of hybrid and electric cars sold worldwide every two months in 2021) resultant wastes would comprise around 250’000 tonnes and half a million cubic metres of unprocessed pack waste, when these vehicles reach the end of their lives.

Although re-use and current recycling processes can divert some of these wastes from landfill, the cumulative burden of electric-vehicle waste is substantial given the growth trajectory of the electric-vehicle market. This waste presents a number of serious challenges of scale; in terms of storing batteries before repurposing or final disposal, in the manual testing and dismantling processes required (nowadays) for either, and in the chemical separation processes that recycling entails [11].

The resulting quantity of waste that has to be stocked presents some serious issues in terms of safety. The electrode materials in Lithium-Ion batteries (LIBs) are very reactive (for instance, far more reactive than tyre rubber, other material with serious dangers connected with stocking) and without a proactive and economically sound waste-management strategy there are potentially greater dangers associated with stockpiling of end-of-life LIBs. For this reason, it is important to seek solutions to minimize stocking period, reduc-

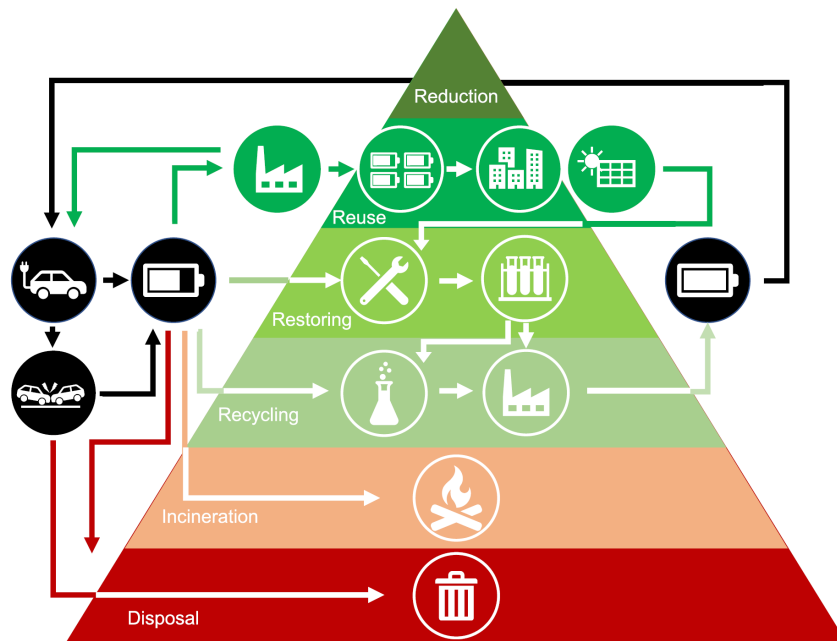


Figure 2.4: End of life batteries management hierarchy.

ing the time required for recycling process, treating higher volumes and finding new reuse solutions.

EV batteries has a life cycle that is estimated to be around 10 years. After this period of time, battery capacity is expected to be significantly decreased, making the battery no longer usable for electric cars, thus arrived at its end of life. However, at the end of the so called "first life", the battery could still be reused, depending on its conditions, for a "second life".

When battery pack reaches its EOL, there are 4 possible paths that can be taken:

- Re-use
- Recovery
- Recycling
- Disposal or incineration

In sustainability terms, this options have different ecological footprints. It is therefore preferable reuse to other methods, and the disposal should only be considered in case of no other options available. Figure 2.4 schematically reports this hierarchy, focusing on batteries recycle, main goal of this project.

For the moment also the economics of the decision whether to recycle or re-use are set firmly in favour of re-use. The main factors are:

- the refurbishment cost of putting the battery into a second-use application
- any credit that would accrue as the result of recycling the battery instead

Nevertheless, although reuse is the preferred way, it is not always possible, both due to the conditions in which the battery packs could be (not suitable for second uses), and due to the possible lack of demand for other applications.

Furthermore, even if batteries are suitable to be reused, after the end of their second use recycling must be the ultimate fate of all LIBs.

In such scenarios, spent batteries may also present an opportunity for manufacturers, as they require access to strategic elements and critical materials for key components in electric-vehicle manufacture: recycled lithium-ion batteries from electric vehicles could provide a valuable secondary source of materials.

2.2.1 Battery recycling

Waste may also represent a valuable resource. Elements and materials contained in electric-vehicle batteries are not available in many nations and access to resources is crucial in ensuring a stable supply chain. End-of-life LIB recycling could provide important economic benefits, avoiding the need for new mineral extraction and providing resilience against vulnerable links and supply risks.

In the future, electric vehicles may prove to be a valuable secondary resource for critical materials (such as Copper, Lithium, Cobalt and Nickel), and it has been argued that high-cobalt-content batteries should be recycled immediately to bolster cobalt supplies.

If tens of millions of electric vehicles are to be produced annually, careful husbandry of the resources consumed by electric-vehicle battery manufacturing will surely be essential to ensure the sustainability of the automotive industry of the future, as will a material and energy efficient "3R system" (reduce, re-use, recycle).

Recycling may involve different phases [11]:

- **Pyrometallurgical recovery**

Pyrometallurgical metals reclamation uses a high-temperature furnace to reduce the component metal oxides to an alloy of Co, Cu, Fe and Ni. The high temperatures involved mean that the batteries are ‘smelted’, and the process, which is a natural progression from those used for other types of batteries, is already established commercially for consumer LIBs. It is particularly advantageous for the recycling of general consumer LIBs, which currently tends to be geared towards an imperfectly sorted feedstock of cells (indeed, the batteries can be processed along with other types of waste to improve the thermodynamics and products obtained), and this versatility is also valuable with respect to electric vehicle LIBs. As the metal current collectors aid the smelting process, the technique has the important advantage that it can be used with whole cells or modules, without the need for a prior passivation step. The products of the pyrometallurgical process are a metallic alloy fraction, slag and gases. The gaseous products produced at lower temperatures (<150 °C) comprise volatile organics from the electrolyte and binder components. At higher temperatures the polymers decompose and burn off. The metal alloy can be separated through hydrometallurgical processes (see section ‘Hydrometallurgical metals reclamation’) into the component metals, and the slag typically contains the metals aluminium, manganese and lithium, which can be reclaimed by further hydrometallurgical processing, but can alternatively be used in other industries such as the cement industry. There is relatively little safety risk in this process, as the cells and modules are all taken to extreme temperatures with a reductant for metal reclamation—aluminium from the electrode foils and packaging is a major contributor here—so the hazards are con-

tained within the processing. In addition, the burning of the electrolytes and plastics is exothermic and reduce the energy consumption required for the process. It follows that in the pyrometallurgical process there is typically no consideration given to the reclamation of the electrolytes and the plastics (approximately 40–50 per cent of the battery weight) or other components such as the lithium salts. Despite environmental drawbacks (such as the production of toxic gases, which must be captured or remediated and the requirement for hydrometallurgical post-processing), high energy costs, and the limited number of materials reclaimed, this remains a frequently used process for the extraction of high-value transition metals such as cobalt and nickel.

- **Physical separation**

After shredding, the materials are subjected to a physical materials separation. During this phase, recovered materials can be subjected to a range of physical separation processes that exploit variations in properties such as particle size, density, ferromagnetism and hydrophobicity.

These processes include sieves, filters, magnets, shaker tables and heavy media, used to separate a mixture of lithium-rich solution, low density plastics and papers, magnetic casings, coated electrodes and electrode powders.

The result is generally a concentration of electrode coatings in the fine fractions of material, and a concentration of plastics, casing materials, and metal foils in the coarse fractions. The coarse fractions can be put through magnetic separation processes to remove magnetic material such as steel casings and density separation processes to separate plastics from foils. The fine product is referred to as the ‘black mass’, and comprises the electrode coatings (metal oxides and carbon).

- **Hydrometallurgical metals reclamation**

Hydrometallurgical treatments involve the use of aqueous solutions to leach the desired metals from cathode material. By far the most common combination of reagents reported is H_2SO_4 and H_2O_2 . A number of studies have been carried out in order to determine the most efficient set of conditions to achieve an optimal leaching rate. These include: concentration of leaching acid, time, temperature of solution, the solid to-liquid ratio and the addition of a reducing agent. In most of these studies, it was found that leaching efficiency improved when H_2O_2 was added.

- **Direct recycling**

The removal of cathode or anode material from the electrode for reconditioning and re-use in a remanufactured LIB is known as direct recycling. In principle, mixed metal-oxide cathode materials can be reincorporated into a new cathode electrode with minimal changes to the crystal morphology of the active material. In general, this will require the lithium content to be replenished to compensate for losses due to degradation of the material during battery use and because materials may not be recovered from batteries in the fully discharged state with the cathodes fully lithiated. So far, work in this area has focused primarily on laptop and mobile phone batteries, as a result of the larger amounts of these available for recycling, but this technique could be also suitable for electric vehicle batteries in near future.

2.3 Cognitive Robotics

As discussed in the report introduction, and further detailed in the previous paragraph, resistive discharge has a number of advantages over other discharge methods. The possibility of recovering the energy stored in the batteries, the absence of contraindications from the environmental point of view and the speed and safety of the entire process, make it an ideal method of discharge. The only weak point consists in the need for intervention by a human operator, in order to connect the battery to the discharge station. With regard to the batteries of electric vehicles, in which high voltages are involved, this represents a significant human safety issue. For this reason, automating the process of electrical connection to the battery pack results to play a very important role.

For this kind of tasks, traditional robotic is not sufficient. The variability of the conditions makes it necessary to have a flexible system, which can adapt to different conditions. To do this, the system is required to have intelligence, to make decisions, and to be able to recognize the environment and make decisions basing on it.

When thinking about end-of-life battery packs it has to be taken into account that there are variations and uncertainties caused by the use of the product, and this has its consequences. In order to solve or minimize to the maximum these uncertainties, the discharge and disassembly performed by the automatic station has been implemented following the principle of cognitive robotics.

In general terms, cognitive robotics is a multi-disciplinary science that draws on research in adaptive robotics as well as cognitive science and artificial intelligence, and often exploits models based on biological cognition.

Cognitive robots achieve their goals by perceiving their environment, paying attention to the events that matter, planning what to do, anticipating the outcome of their actions and the actions of other agents, and learning from the resultant interaction. They deal with the inherent uncertainty of natural environments by continually learning, reasoning, and sharing their knowledge.

A key feature of cognitive robotics is its focus on predictive capabilities to augment immediate sensory-motor experience. Being able to view the world from someone else's perspective, a cognitive robot can anticipate that person's intended actions and needs. This applies both during direct interaction (e.g. a robot assisting a surgeon in theatre) and indirect interaction (e.g. a robot stacking shelves in a busy supermarket).

In cognitive robotics, the robot body is more than just a vehicle for physical manipulation or locomotion: it is a component of the cognitive process. Thus, cognitive robotics is a form of embodied cognition which exploits the robot's physical morphology, kinematics, and dynamics, as well as the environment in which it is operating, to achieve its key characteristic of adaptive anticipatory interaction [12].

According to the paradigm of cognitive robotics, on this project are integrated different technologies, in order to achieve environmental detection, robot physical interaction and decision making:

- Anthropomorphic robotic arm
- Computer vision system
- Artificial intelligence

Chapter 3

Methods

This chapter reports the theoretical treatment of all the "tools" used for the realization of this project. In addition, the steps necessary to carry out each experimental test are explained in detail and commented on. For the test results, refer to the chapter 5, number 5 of this report.

3.1 Discharge Strategy

The hierarchical structure of the battery pack, divided into modules, consisting of series connected cells, give the possibility of choosing between many different discharge strategies.

By "discharge strategy" is meant the methodology that will be used for the discharge process of the battery pack. In particular, it's necessary to choose which level to act the discharge: pack, module or (theoretically) cell. Once decided, it's necessary to access that level and connect the cable for the discharge.

Naturally, discharging on a deeper level (module or cell) requires previous dismantling of the pack to access the terminals, but leads advantages simplifying and making safer the discharge; on the other side, moving the process on a higher level (battery pack) reduces the required times (no dismantling needed) but make it less safe and more complex to manage.

Choosing the discharge strategy is the first step to take on the development of this project, and the entire subsequent design of the discharging station, will be based on this choice, so it's very important to chose the most proper one, considering all the trade-off aspects that will be shown below.

3.1.1 Trade-off Aspects

There are four main aspects that have to be considered when planning the discharge strategy, which can be summarized in:

- Time to Discharge
- Safety on Discharge
- Complexity of the Operation
- Flexibility of the System

These four aspects are related between them, and acting on one imply changes on others. For this reason a good trade-off is needed to ensure an optimal solution for the overall system.

Time to discharge

By "discharge time" is meant the overall time required to complete the discharge of the entire battery pack, from the moment when the discharge starts, to the moment when all modules reaches final values of SOC and voltage.

This means that if the discharge strategy expect to discharge modules separately, also the time required to move from one module to the next will be taken in account when calculating the discharge time. Considering this, it follows that the lower in the hierarchy level the discharge is carried out, the greater will be the overall discharge time. Therefore, discharging at the cell level will take longer than discharging the entire pack in a single operation, because in addition to the time required for the electric discharge of the batteries, it will take a certain time to pass from one cell to the next.

Discharge time, obviously, is expected to be as short as possible. During this process no other dismantling operation can be performed (for safety reasons, discharge batteries is one of the first step taken during the EVB dismantling industrial process), so it's crucial to keep it as low as possible.

Safety on discharge

Safety it's a parameter that could not never be lacking. For this reason, any discharge strategy (have to) guarantee the minimum safety standards.

Thus, when comparing different discharge strategies, "safety on discharge" means the set of various safety related parameters. The amount of voltages involved in the process, directly related to the discharge strategy, it's the critical aspect when talking about safety.

In general, discharge batteries connecting to the lower levels of the hierarchy (i.e., modules) it's safer, because lower voltages are involved and it's easier to monitor and control single modules. Contrarily, discharge connecting to higher hierarchy level (i.e., pack terminals) involves higher voltages and make monitoring of single modules more difficult. Higher voltages increase potential risks during the discharge process (higher currents and heat generation), and so more complexity is required to the discharge circuit in order to handle the process safely.

Safety, of all, is the only parameter that cannot be missing, it must be guaranteed above all other needs, therefore, whatever strategy is chosen, it must guarantee the safety of the operation.

The first determining factor for safety, however, is how this is done, so regardless of the level at which the discharge is performed, the current determines the safety of the operation.

System complexity

A discharge strategy that involves hacking the BMS is inherently more complex than one that does not. Complexity therefore refers to the "number of operations" required to achieve the discharge target.

The more complex the system, the less flexible it is. In fact, if it is required to find and use the specific CAN commands for a certain battery pack, these will not work on another one, and the developed system will not be able to adapt to a different battery packs.

Furthermore, complexity leads to more time required to implement the system, which would need more setup time, that is not preferable in industrial application.

Flexibility of the system

Flexibility is the capability of the system to adapt to different battery packs from different manufacturers.

If complexity increase too much, the system tend be too tied to the single battery pack that it has been designed for. Simpler systems are instead easier to modify and adapt to operating conditions different from those of the project, if necessary.

3.1.2 Technical Limits

On a theoretical level, the discharge could be acted at each one of the three levels: cell, module and pack. Nevertheless, in practice, this is not really possible, due to the too deep dismantling level that this discharge strategy would require, in order to access cell terminals.

On the previous section, all the theoretical pros and cons have been discussed, however, we have to consider also some practical limits, that may set some constrains to what is possible to do. The main aspects to consider are the Battery Management System (BMS) and the Battery Junction Box (BJB). This devices are always present in an EV battery packs, and are essential for the functioning of the battery during its life cycle. The BMS carries out a series of monitoring and control functions of cells and modules, to ensure their balance, correct and uniform charge and discharge and other features related to safety. Further safety features are ensured by the BJB, which acts as an interface between battery pack and vehicle. It contains the "switching unit" of the battery pack, and directly connects the modules to the external high-voltage connector, where is plugged the power supply cable of the car. The BMS sends control signals to the BJB, deciding the switch configuration, i.e. to open or close the electrical connection to the external. For safety reasons, the BJB's switch is normally open, so when the car is turned-off (or the battery is unplugged from the car, as in our condition) the high-voltage power supply is disconnected. This is a problem for our purpose: if we want to discharge at pack level we would need to have a closed switch, so as to be able to connect directly to the external socket and discharge the entire battery at once. The presence of the BJB precludes, then, the discharge strategy acted on the pack level. To avoid this, and make possible also that discharge strategy, two solutions are proposed:

- Battery Management System hacking
- Battery Junction Box bypassing

The Battery Junction Box is the part where the circuit is physically open. In order to realize the discharge, we need to connect, through cables, the battery to the discharge device , but even if connected it is not possible to start the discharge process until the

circuit is open. The first solution, consist of closing the switch to allow the current to flow. To achieve this, the only way is to send a control signal that closes the contact. All car electronic components, battery parts included, are connected via CAN-bus, as shown in figure 3.1, hence that's the network we have to use to communicate to the battery junction box. BMS is the unit that controls the BJB, thus, we need to access the BMS and set that switch to open. Unfortunately, automotive manufacturers do not provide the CAN-bus commands needed to control their devices, due to the strict industrial secrecy necessitated by companies competition. Lacking official documentation, the only way is to hack the system, through unofficial resources and making tests at the lab, to find a working commands configuration. This route, however, has a number of disadvantages. First of all, the high laboriousness and complexity: obtaining the correct commands is not easy, it would require many hours of research in the laboratory and several attempts, without even the guarantee of obtaining a result. Then, specific tools are required to connect to the CAN BUS network, which would increase the overall cost of the station, but mostly would make it more complex to integrate a system of this type into a fully automatic station, especially due to the difficulty of connecting the instruments to the battery network. Furthermore, with new battery packs developments, commands may change, making obsolete and not working the previously found ones, or anyway commands may vary between different battery models, a specific study for each one would be necessary. This lack of flexibility, it would require an ad-hoc built system for each battery, is not wanted in industrial automation. Another aspect to take into consideration is that we do not know in advance the state of the battery pack, it could come from a damaged car and some parts, like the BJB or the BMS, could be not working properly, which would make this technique not applicable. For the previously discussed reasons, the first option, hacking the BMS, has been discarded.

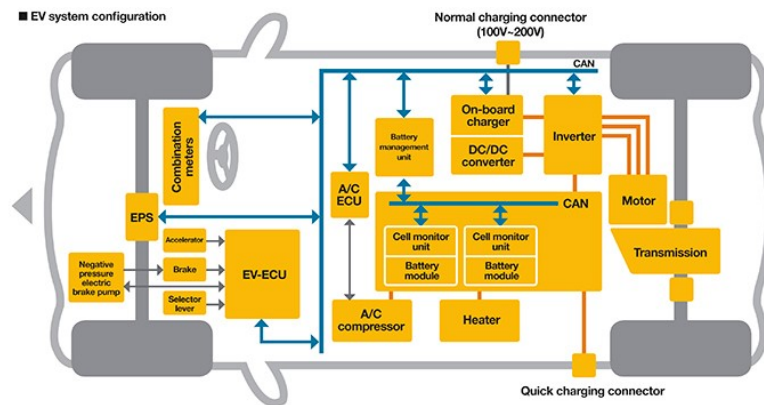


Figure 3.1: Electric vehicles CAN-bus configuration scheme

The second option to allow the discharge at the pack level, is the junction box bypassing. Since it was decided to don't control the BJB, the idea is to simply do not pass the circuit through the switch, which is open. On previous scenario, the discharge device was connected to the battery using pack's socket, which is connected to the junction box, that we now want to exclude. In order to do that, it is necessary to connect the discharge device before the battery cables enter the BJB. Located here, are present two connectors linking the extremities of the series connected modules to the BJB, as highlighted in figure 3.2. Unplugging these connectors from the junction box, is possible to access the whole battery

pack without any safety limit or switch. The connectors have then to be plugged into the discharge device . This operation has to be carried out by a robot arm, automatically, that has to detect the terminals, determine their position, grab and move them to the required position, in order to be connected to the discharge device . This second option has been chosen for the project development, being more feasible to act, more adapt to the problem and doesn't require any particular tool, also making the system more flexible, possibly able to adapt to different battery models in case of further upgrades.

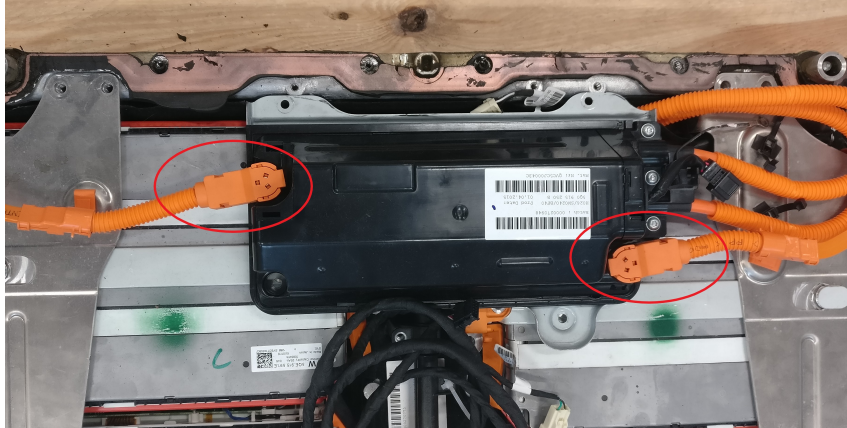


Figure 3.2: Battery Junction Box (BJB) connectors

3.2 YOLO

When talking about object detection, it is important to clarify the concepts of image classification and object localisation. Image classification, refers to a computer vision process that is able to classify an image according to its visual content. Then, object localisation allows to detect the specific position of the object in the image. Object detection, basically provides the tools for finding all the objects (in this case the components) in one image, and drawing the bounding boxes around them. Finally, image segmentation is able to define the contours of the detected objects.

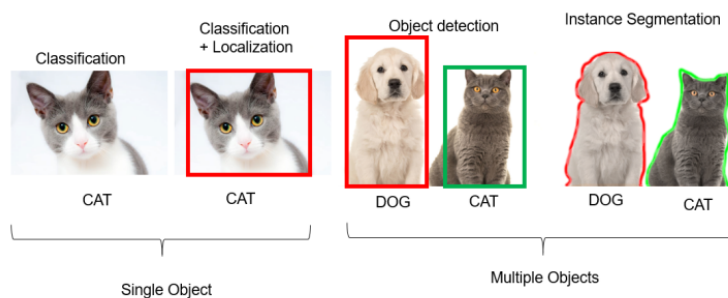


Figure 3.3: Differences between image recognition methods

Given that the final purpose of the project is to implement the solution to the industry, algorithms based on segmentation have been discarded. This decision is based on that the creation of the training database for this type of algorithms is more complicated. This results on larger procedures to add new models into the known database. When analysing object detection algorithms, they can be generally classified into two groups:

- **Algorithms based on classification:** Implemented in two stages, first, they select the regions of interest (ROI) in the image. Then, they classify these regions using convolutional neural networks (CNN). Since, they have to find the ROI of the image, the solution can be slow.

One of the most representative algorithms of this type are the Region-based Convolutional Neural Network algorithm (RCNN, Fast-RCNN, Faster-RCNN and Mask-RCNN) and the RetinaNet algorithm.

- **Algorithms based on regression:** Instead of predicting the Regions of Interest of the image, this type of algorithms predict classes and bounding boxes for the images in one run. Within the well-known algorithms of this group, there are the You Only Look Once (YOLO) family algorithms and SSD (single Shot Multibox Detector).

In this project, the You Only Look Once (YOLO) version 3 has been selected as algorithm for the object detection part. YOLO is a real-time object detection algorithm. It is based on a convolutional neural network, and as explained before, it is an algorithm based on regression. Thus, the algorithm applies a single neural network to the full image.

The image is divided into smaller regions on which the bounding boxes (and the probabilities) are predicted for each region. These predicted probabilities weight the bounding boxes.

YOLOv1 was the first version of the algorithm. This version had 26 layers in total, with 24 Convolution Layers followed by 2 Fully Connected layers, but the main problem with YOLOv1 was its incapacity to detect tiny objects. Then, in December 2016, the paper 'YOLO 9000: Better, Faster, Stronger' by Redmon and Farhadi was released. A lot of improvements were included in the second version of the algorithm. Finally, in April 2018 the same researchers published 'YOLOv3: An Incremental Improvement', introducing important changes that significantly improved YOLO capabilities. This final version no longer copes with small objects and runs significantly faster than other detection methods.

The algorithm only requires one forward propagation pass through the neural network to obtain the predictions. Then, to detect only one time each object, a non-max suppression is done. In that way, the algorithm returns the detected objects with the bounding boxes and the probabilities.

Using YOLO algorithm, an individual convolutional neural network is able to predict multiple bounding boxes and the 5 corresponding probabilities for them. YOLO trains on full images and directly optimizes detection performance.

The system uses dimension clusters as anchor boxes to predict the bounding boxes. Four coordinates (t_x , t_y , t_w and t_h) are predicted for each bounding box. Therefore, if the previous bounding box has width and height (p_w and p_h) and the cell is displaced by (c_x and c_y) from the top-left image corner. The predictions are:

$$bx = \sigma(t_x) + cx$$

$$by = \sigma(t_y) + cy$$

$$bw = p_w e^{t_w}$$

$$bh = p_h e^{t_h}$$

Then, the algorithm predicts, using logistic regression, an objectiveness score for each bounding box. If the bounding box is overlapping the ground truth object 2, the score has a value of 1. If a bounding box is overlapping a ground truth object, but the score is not the best, it is ignored.

Later, to realize the class definition, the algorithm predicts the classes that a bounding box can contain using multi-label classification. A multi-label approach gives better results than other classifiers for applications where there are many overlapping labels.

YOLOv3 is trained on full images with no hard negative mining. To train YOLOv3, it is used: multi-scale training, data augmentation and batch normalisation (within other standard procedures). The open-source neural network Darknet is used for training. Darknet is written in C and CUDA and supports CPU and GPU computation.

3.3 Training phase

The first phase to carry out in a YOLO algorithm implementation, is the convolutional neural network training. To learn how to act object detection, the network needs to study a big amount of data, from which it must obtain operational information. In this case, the data are images taken in real operational environment, thus a set of images of the battery pack that will have to be analysed. This pictures, must contain information useful for the network in order to detect the terminals, they must therefore be labeled images.

3.3.1 Images acquisition

Together with the BB, another, even more important, aspect to take care of when preparing the images for the network training, is the variety of pictures selected. A very important aspect to take care of when preparing the images for the network training, is the variety of pictures selected. Indeed, it is crucial to provide the algorithm with an heterogeneous set of images, which deduce different information from. If this is not done, and for training are used only pictures taken in the same conditions, the CNN (in operating conditions, after being trained) will be limited to perform object detection only in that conditions, and if these change, it won't be able anymore to achieve its tasks, or anyway will get worse performances. As already said, to avoid this excessive specificity, a diverse images collection is preferable. The more various the set, the more capable of detecting in diverse conditions the algorithm will be, increasing adaptability, a fundamental aspect when talking about artificial intelligence.

In industrial operations, the different conditions, that is referred to above, may include:

- Different brightness of the environment, depending on which part of the day the plant is working:
 - During day-time: natural light, it changes based on what time it is, can be stronger or weaker
 - During night-time: artificial lighting, brightness is constant, but it's a different type o light compared to the natural one
- Different points of view from which to take the picture, there can be different:

- Angles: due to different reasons¹, the angle² between the camera and the subject of the picture (the battery pack in this case) may be little different from case to case.
- Distances: for the same reasons, the distance between the camera and the subject can change considerably.

When taking the pictures to make the training set, has been taken care in creating images with regards to each of these parameters. This means that pictures has been taken with different lighting conditions, during different times along the day, from different points of view for angles and distances, moving the robot arm around the robot.

For the training, a set of all different pictures is taken, according to the criteria exposed above. After labelling, all the images were given to the algorithm to begin the training phase.

3.3.2 Image labeling

Together with the picture variety, another very important aspect to take care of when preparing the images for the network training, is the image labelling. Image labeling is the process of identifying and marking various details in an image. It is a fundamental step in every automated image recognition system, and the accuracy with which this phase is carried out, directly determines the accuracy of the algorithm in being able to recognize and precisely locate objects.

The main objective of labeling the pictures is to let the algorithm know where the battery connectors are located in the image. The algorithm takes these images and extracts the features of the labeled areas in order to learn how the different objects are and how to detect them. On a visual level, the labels are represented as so-called "Bounding Boxes" (BB), that are squares which, in the image, determine the area within which the object specified is located. As a result, the narrower and more precise around the object the bounding box, the more accurate the bounding boxes generated by the algorithm (once trained and operating) will be, including in the detected area only the object, and not much space or other objects around it. That is, for this project, a very important aspect to take into consideration, since the bounding boxes obtained are used to determine the 3D space location of the connectors.

YOLO protocol, defines that the bounding boxes in the labeled images has to be described by a separate text file (*".txt"* extension), with the same name of the image, to correctly associate the labels for each picture. The file, contains the description of the labels, one for each row, reporting the position of two opposite corners (that uniquely identify a box) and then the class that it belongs to. In general terms, a class is the name by which it has to refer to the labeled object. In this case, there are two different classes:

- left_pole
- right_pole

¹it is possible that the robot is not always starting from the same position due to different operations performed before

²As angle, can be considered the one between the axis radial to the battery pack and the axis exiting the camera lens

That refers to the left and right connectors of the cells series to the battery junction box (further details at page 17 of this chapter).

To create the database for this project, it has been used the open-source program LabelImg. It allows to quickly create labels, using a visual interface that makes it easy to pin the corners of the BB, and automatically creates the text files linked to each photo in the defined YOLO format.

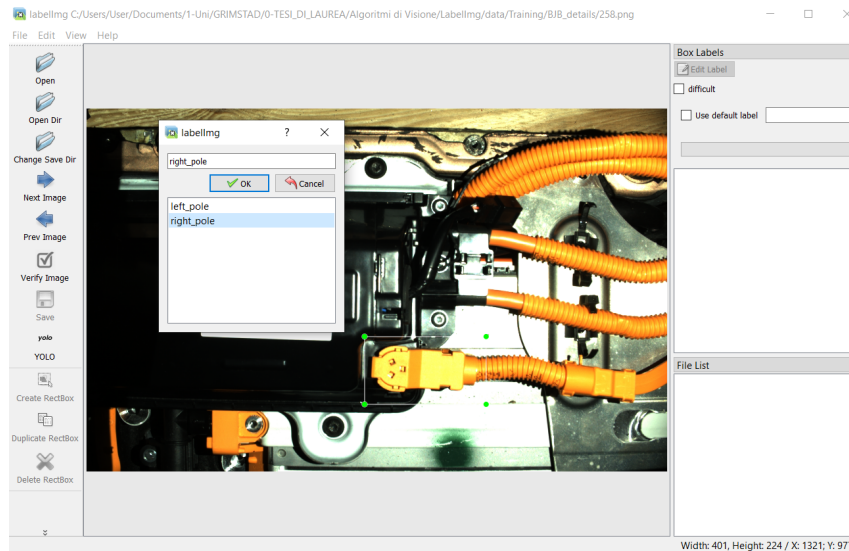


Figure 3.4: LabelImg software interface

The focus of this project is on a single battery pack, of the Volkswagen Passat Hybrid, however, further stages of the project may add also different battery packs, thus requiring an extension of the images database, to allow the network to recognise also different models.

3.3.3 Neural network training

The final step, consists of the actual training phase. In artificial intelligence, "training" refers to the process the neural network needs to learn how to perform its task. During this phase, the network requires a lot of data, together with the "answers" to the goal it has to achieve. From these examples the algorithm learns, thus it sets a series of internal weights on each of its layers, which will later allow the AI to carry out the task independently. The same set of data is analysed many times, and each one serves the network to learn something new, and adjust its weights. A cycle takes the name of epoch. To obtain better results in training a neural network, many epochs are always necessary. More epochs requires more time

Training requires always a lot of time, which is directly related to the number of epochs. However, more epochs leads better performances once the network is trained, thus is always preferable to spend more time in training and obtain better results when it is operating. On the other side, the number of epochs can't be too high, otherwise there is a risk of running into a problem called *overtraining* or *overfitting*. Overfitting happens when the model fits too well to the training set. It then becomes difficult for the model to generalize to new cases that were not in the training set, thus it's not able to act object detection on images different from the ones contained into the training set. To avoid it, it is necessary to train the model with an appropriate number of epochs, with a balanced trade-off between

accuracy and generalization. YOLO gives some output parameters in terms of loss values and evaluation metrics in order to evaluate the training and avoid overfitting.

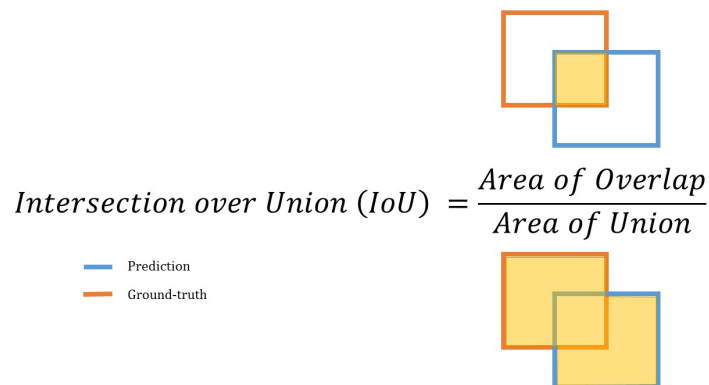
To find an appropriate number of epochs, training has been performed many times, making different test varying the number of epochs. The comparison between different tests can be done in different ways: comparing output parameters of the training and, in a more practical way, testing the resulting network weights in an operational case, thus acting some detections. Both are used for the comparison in this project (results reported in chapter 5).

There are seven main parameters that YOLO gives as output in order to evaluate the training executed, that are:

- **Intersection over Union (IoU)**

IoU, also known as the Jaccard index, is the most popular evaluation metric for tasks such as segmentation, object detection and tracking. Object detection consists of two sub-tasks: localization, which is determining the location of an object in an image, and classification, which is assigning a class to that object. Therefore the goal of localization in object detection is to draw a 2D bounding box around the objects in the scene. The ground truth is the box containing the object which has to be detected (obtained from the labeled data used for training). On the other side, the output of the neural network is called prediction bounding box, and contains the localization of the object according to the CNN.

We want to evaluate the accuracy of this prediction. The IoU is calculated as follows:



$$\text{Intersection over Union (IoU)} = \frac{\text{Area of Overlap}}{\text{Area of Union}}$$

— Prediction
— Ground-truth

Intersection over union index has the appealing property of scale invariance. This means that the width, height and location of the two bounding boxes under consideration are taken into account. The normalized IoU measure focuses on the area of the shapes, no matter their size.

Starting from IoU an improvement of this index is the GIoU: Generalized Intersection over Union. It is obtained considering not only the overlap between the boxes but also how far the prediction is from the ground truth [27]:

$$GIoU = IoU - \frac{|C \setminus (A \cup B)|}{|C|}$$

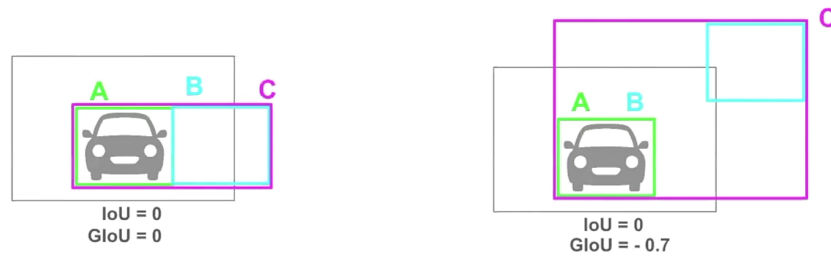


Figure 3.5: Generalized Intersection over Union (GIoU).

Both IoU and GIoU are supposed to converge to value 1, as the bounding box prediction gets better. These parameters are often used to evaluate predictions during training in order to distinguish wrong from correct ones (verifying if their IoU/GIoU value goes beyond a given threshold).

- **Objectness**

Objectness is essentially a measure of the probability that an object exists in a proposed region of interest (i.e. in a prediction bounding box). If there is high objectness, this means that the image window likely contains an object. This allows us to quickly prune out proposed image windows that do not contain any objects.

The opposite case is represented by the "No Objectness", which calculates the probability that there is no object into the bounding box. Ideally, to produce a better result of localization, the two parameters should reach complementary values:

$$Obj \rightarrow 1 \quad No\ Obj \rightarrow 0$$

- **Classification**

Classification is the process of associating an object to its own class, thus the algorithm identifies what is contained into a certain area. "Classification" YOLO's output parameter refers exactly to this. It indicates the correctness of object classification to respective classes, where the value is expected to approach 1 as the number of epochs increases.

$$Class \rightarrow 1$$

The parameters shown above give an information about how YOLO is performing the training along epochs, defining if it is actually learning or not, and detecting possible overtraining, when calculated on the detection set.

The remaining parameters are instead called "evaluation metrics", and have the aim of evaluating the network performances on identification along epochs. They are:

- **Precision**

It measures how accurate is the predictions, i.e. the percentage of predictions that are correct (called true positives, TP) on the total amount of predictions done, which includes the wrong predictions (called false positives, FP).

It can be measured as:

$$Precision = \frac{TP}{TP + FP}$$

- **Recall**

It measures how good is the network in finding all the objects within the image. Are called "false negative" (FN) the objects that the network doesn't detect.

$$Recall = \frac{TP}{TP + FN}$$

- **mAP**

Average precision (AP) is defined as the area under the precision-recall curve. The mean average precision (mAP) is the average of AP calculated for different IoU thresholds.

- **F1**

It is a parameter the merge together precision and recall, giving an idea of their balance. It is calculated as the harmonic mean of precision and recall:

$$F1 = 2 \frac{precision \cdot recall}{precision + recall}$$

3.4 Detection phase

Once trained, the network is ready to perform object detection. Detection is the process, performed by the vision algorithm (YOLO), of identification and localisation within the image of the classes it has been trained for. The network is capable of drawing a bounding box around each one of the objects detected, together with the name of the object, and the confidence percentage. This value is in the range of 0 to 1, and represents the probability, according to YOLO, that the identification is correct. A typical object detection result can be like the one reported below (figure 3.6).

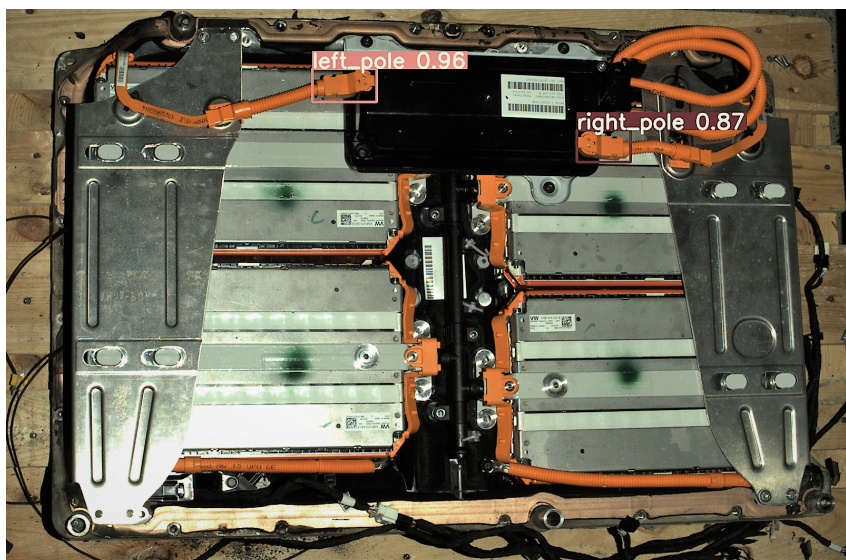


Figure 3.6: A typical YOLO detection, reporting bounding boxes and confidence percentage.

Figure 3.6 reports a detection performed successfully, where connectors are correctly identified and located. As shown, different bounding boxes may have different confidence percentage.

With "detection phase" is meant the operations of test of the weight configurations found, to evaluate its effectiveness and eventually re-train the model, in case of not satisfying performances. It's clear that at the beginning it's necessary to pass from this phase to the previous one (training phase) many times, to try different configuration, until the best weights are found.

The weights configuration under test has to be tried on a representative set of images, according to the parameters explained at page 23. The network will identify within every picture the objects it was trained for, drawing a bounding box around them, and without knowing a priori the number of objects in the picture.

To evaluate the quality of a detection, there are some characteristics that have to be considered:

- Recognition of objects presence
- Number of objects detected compared to the real number
- Location of the BB compared to the real object
- Area of the BB relative to the size of the object (detection accuracy), which can be smaller or wider
- Association between detected objects and the correct belonging class
- Confidence percentage of each detection
- Wrong identifications

These considerations allow to compare different weights objectively, in order to identify which is the best configuration.

The comparisons in question, with relative results, are reported in chapter 5.

3.5 Batteries discharge

Discharge batteries is not an easy task. There are many factors that come into play, and adjusting them properly determines the success of the discharge. The parameter that have to be taken into account are:

- Discharge current
- Cell voltage
- Cell temperature
- Discharge time

Changing one of this parameters, has effects on the others, therefore it is necessary to find a trade-off, depending on what is the objective. During their life-cycle, batteries are used as a portable power supply, for this reason, the goal is to make the discharge process last as long as possible. In this project, instead, batteries are at the end of their life-cycle, and the objective is to discharge them to be recycled. For this reason, the discharge has to be as fast as possible, and the parameter that directly determines discharge time, is the

discharge current, that has to be very high. Nevertheless, as said before, all the aspects are connected, and the current is also directly related to the temperature of the cell. Together with the rising temperature, a number of serious effects can occur, leading to problems such as chemical deterioration of the cell, overheating, but also fires and explosions. The temperature of the cell represent therefore the main limit to the discharge current, and then to the discharge time.

The objective of this project is to design an automatic station for batteries discharge, which is the first step to take on the process of recycling an electric vehicle battery packs. Being the goal the recycling, not the reuse, it is not important that cells are not damaged during the process, they will not be used anymore, but shredded to extract their basic chemical elements. For this reason, it is not necessary to stop at the cell cut-off voltage, chemical degradation or capacity loss are not an issue.

The unique phenomenon that needs to be worried about, for safety reasons, is overheating. Indeed, during the discharge process, high discharge current may generate huge amounts of heat, that may trigger fires or, in the worst cases, even explosions. It is then important to act a strict control of the temperature during the discharge process.

Nevertheless, this is just a case of study. It is not always recycling the destiny of EV batteries at the end of their life-cycle. Electric vehicles need high performing batteries, to always maintain good standards in autonomy, power-train performances and durability. For this high level required, may happen that sometimes a battery pack that is still good preforming in absolute terms, it is considered not performing enough for a car, and it is then replaced. An other possible scenario, is that after a car crash the vehicle is too damaged to be repaired, and is scrapped, but the battery pack may still be intact and perfectly working. In these cases, recycling a still perfectly working battery pack would result to be wasteful; it is thus preferable to reuse it for a second life. In such situations, the same pack, in its original form, can be intended for a different use; alternatively, and more often, the car battery is partially discharged (not down to 0, like in recycling) and dismantled to obtain the single cells, that will be reassembled on a different pack, depending on the chosen next use. There are many possible applications for second-life batteries, such as smart grids, home storage, industries peak shaving, storage of renewable energy and so on, as further explained in document [25].

3.6 Discharge control

Discharge control is the "decision-making process" used to decide what has to be the current value during discharge. Current can be constant or variable, and the temperature can be monitored or not, depending on which control is used. There are three main doable control strategies, that are:

- Open loop control
- Open loop model based control
- Closed loop feedback control

Open loop

Open loop control is the simplest, cheapest and quickest to implement. As an open loop control, it provides that there is no feedback quantity, and thus no sensors to monitor the ongoing process. However, to avoid safety hazards, temperature can't never rise over a safety level. Without monitoring the temp, it is not possible to know its value in real-time, so it's necessary to act with a large safety margin. For this reason, discharge current must always maintain a low value. This leads discharge times to expand considerably, and it is a big drawback.

This is the actually used control in the discharge station that has to be upgraded in this project. It is a low performances approach and thus has to be improved, both in safety and process time.

Model based

Open loop control can be improved introducing a thermal model into the control. The model is a mathematical model that can predict in real-time the thermal behaviour of the battery pack, thus the heat generation and how it effects temperature. As input is given the discharge current, continuously, and the model returns the evolution of the temperature, for each time instant.

The same input (the value of the current) will be given to the control and to the model, and the output of the model is fed back and compared to the reference value, in order to obtain control input. The controller, then, has not a view on what's happening on the real world, but has an estimation of it, given from the model.

The downside of this control is the necessity to find an accurate model of the battery pack, which may not be easy, and that requires not negligible time during the design phase of the control³. Furthermore, it is necessary a very accurate model, otherwise temperature prediction during operation could be wrong, resulting in possible overheating, with all the hazards explained in previous section. Considering possible model inaccuracies, the temp reference given to the control has to have a margin with respect to the real maximum value allowed, and this margin has to be greater the bigger the model uncertainty. Lower temperature means smaller current, and then longer discharge time due to slower discharge.

Another drawback of this control, is that to treat different battery packs (from different manufacturers and different vehicles) it is necessary to find a specific mathematical model for each one, that correctly describes its behaviour. This implies less adaptability of the system, because the station will not be able to treat different battery packs from the ones it has been designed for. Every time a new pack wants to be included, the relevant model, with laboratory experiments, must be obtained. This is an important limit of this control, which can be overcome with a different control approach, the closed loop.

³The eventual model has to be found during the design phase of the control, thus in the laboratory before the station is operating. This means that once the model is found, during normal plant operation, it won't affect working time, but it will require more time in the previous phase, when implementing the control due to the time needed to derive the model.

Closed loop

The last strategy proposed is the closed loop control. It is the most commonly used control in industrial applications and provides that the quantity generated by the process, the output, is compared with the reference and on basing on the error between these, the system is acted upon in order to obtain the desired behavior. In industries, feedback control is often used to increase system performances, and it is appreciated for his high flexibility, being able to adapt to changing situations and eventual non-idealities or mathematical model inaccuracies.

As said before, in this application temperature is the unique parameter that limit and thus determine the discharge current. It is therefore immediate that it is the quantity to be used for the feedback. Compared to the other options, this control, offers a number of advantages. Firstly, it is the unique control that physically has a direct view on the real battery, a great safety advantage, which also allows to push further the system dynamic, having smaller errors on knowledge of temperature. Furthermore, it is fast to implement, since it doesn't require various model characterization for different battery packs. Once correctly initialized, it is capable of adapt to different battery models, just reading real-time temperature, and without requiring any change. Also eventual small errors during the tuning phase can be handled by the feedback, resulting in a very robust system, important quality in industrial practice.

However, the most important characteristic of this control, is that it's the fastest and best dynamic performing between the ones considered, drastically reducing discharge time. Indeed, thanks to the feed-back control performed on the real (unless not decisive inaccuracies due to the measurement) value, it is possible to set the reference to higher levels, since the control will precisely keep the temperature below it. This is different compared to model-based control, where it was necessary to reserve a safety margin between reference and maximum allowed temperature, to compensate for any model inaccuracies.

The implementation provides that a reference temperature is set, which is the maximum reachable value staying in safe conditions. This is compared with the measured one, and making the difference between terms it's found the error. A PID controller take that error as input, and generate an output in order to reduce it down to zero. The output is the discharge current, imprinted on the physical system by a variable load.

At this point, the control is ready, and just need a measure system capable of reading the battery temperature. For this purpose, a thermal imager is integrated into the system.

3.7 Thermal Imaging

As explained in the previous section, a closed loop feedback control is chosen, it is thus necessary a sensing system for battery temperature.

Of all of the industrial sensing technologies, temperature sensing is the most common. This phenomena can be explained by citing examples in a multitude of applications where knowing and using the actual or relative temperature is critical. For instance, other sensors such as pressure, force, flow, level, and position many times require temperature monitoring in order to insure accuracy. For this reason, there are many available technologies to perform temperature detection, basing on specifics of the problem.

The most popular temperature sensors used today are the Thermocouple, Resistive Temperature Device (RTD), Thermistor, and the newest technology, the Integrated Silicon Based Sensors. Are also very common other sensing technologies, such as Infrared (pyrometers and cameras) and Thermal Pile.

Each of these sensor technologies cater to specific temperature ranges and environmental conditions. The sensor's temperature range, ruggedness, and sensitivity are just a few characteristics that are used to determine whether or not the device will satisfy the requirements of the application. No one temperature sensor is right for all applications, but it depends on the specific case [2].

Table 3.1 summarizes the main characteristics of these temperature sensors.

For the purpose of this project, it is necessary to have a real-time detection of the temperature on the whole battery pack. All the technologies exposed above are suitable for it, however, thermocouples, RTDs, thermistors and silicon based sensors, can detect temperature on a single point and needs to be in contact, or very close, to the target. To entirely monitor a big object, like the battery pack is, many of them would be required, disposing a "network" of sensors with a sufficient density to obtain a full view on the pack. For its complexity, and thus the difficulty to be implemented in an automated system, this is not a convenient approach.

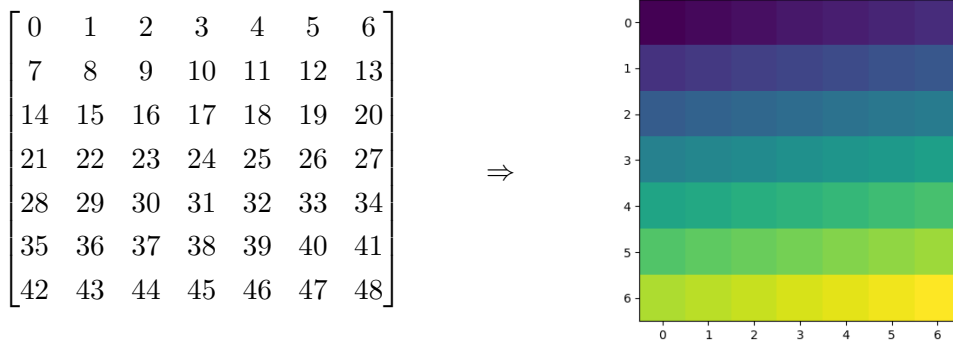
The best option is thermography. Without the need for any physical contact with the object to be measured, it's immediate to adapt to different battery packs, and it's easier to integrate in a robotic system. Thermography offers two solutions: pyrometers and cameras. Pyrometers is another name to refer to infrared thermometers. They can precisely detect temperature, with a wide working range, and in short time, making them suitable for industrial automated application. Nevertheless, they work on a single spot, it is therefore not possible to entirely monitor the battery pack at once. As a matter of fact, also in this case it would be necessary a network of sensors to monitor the pack in different points, to obtain the overall view wanted.

The motivations explained above, show that for the station designed in this project, the best solution is a thermal camera. Having a total view on the pack, it is easy to spot eventual overheating and locate its position, and the full pack can be monitored with just one sensor. It is also immediate to adapt to different battery packs, for model, structure, typology and size, as long as they fit into the field of view (FOV) of the camera.

The output is a matrix of 160 rows by 120 columns, each one containing the temperature measurement of the area located in that position on the camera FOV. This matrix can be colorized. Each measurable value is associated with a certain unique color, assigned following the order of the chromatic scale from blue to yellow for the increasing values: low temperatures are associated with the blue color, and increasing values the hue progressively changes towards yellow. An example of how this process transforms matrices into images is shown below:

Thermocouple	<p>It consists of two wires of dissimilar metals that are soldered together at one end. The temperature at the Reference Junction (also known as the Cold Junction Compensation Point) is used to negate the errors contributed by the Iron-Copper and Constantan-Copper junctions. The connecting point of the two metals of the thermocouple is positioned on the target where the temperature measurement is needed. This configuration of materials produces a voltage between the two wires at the unsoldered end that is a function of the temperature of all of the junctions, consequently, the thermocouple does not require voltage or current excitation. As a matter of fact, an attempt to provide either type of excitation could introduce errors into the system. The termination ends of the thermocouple wires connect to another metal, usually copper. This creates another pair of thermocouples, which introduces a significant error to the system. The only way to negate this error is to sense the temperature at the Reference Junction box (another point on the copper plate, not in between the two junctions) and subtract the contributing errors of these connections in a hardware solution or a combination of software and hardware. Thermocouples are highly non-linear and require significant linearization algorithms, performed on both software and hardware components. In principle, it can be made from any two metals, however, in practice there are standard combinations because of their qualities of linearity and their voltage magnitude drop versus temperature.</p>
RTD	<p>The RTD (Resistance Temperature Detector) is a resistive element constructed from metals, such as, Platinum, Nickel or Copper. The particular metals that are chosen exhibit a predictable change in resistance with temperature. Additionally, they have the basic physical properties that allow for easy fabrication. The temperature coefficient of resistance of these metals is large enough to render measurable changes with temperature. The linear relation between resistance and temperature of the RTD simplifies the implementation of signal conditioning circuitry.</p>
Thermistor	<p>If accuracy is a high priority, the thermistor should be the temperature sensor of choice. The NTC (negative temperature coefficient) thermistor is constructed of ceramics composed of oxides of transition metals (manganese, cobalt, copper, and nickel). With a current excitation the NTC has a negative temperature coefficient that is very repeatable and fairly linear.</p>
Integrated silicon	<p>The silicon temperature sensor is an integrated circuit, it therefore ease of installation in the PCB assembly environment. Integrated circuit designs can be easily implemented on the same silicon as the sensor. This advantage allows the placement of the most challenging portions of the sensor signal conditioning path to be included in the IC chip. Consequently, the output signals from the sensor, such as large signal voltages, current, or digital words, are easily interfaced with other elements of the circuit. On the other hand, the accuracy and temperature range of this sensor does not match the other types of sensors discussed above in this table.</p>

Table 3.1: Main temperature sensing technologies overview.



At this point, by interpreting the matrix as an image, as if each of its elements were a pixel, a visual representation of the temperature on the battery pack is obtained. Figure 3.7 shows a generic example in which this technique has been applied. This kind of repre-

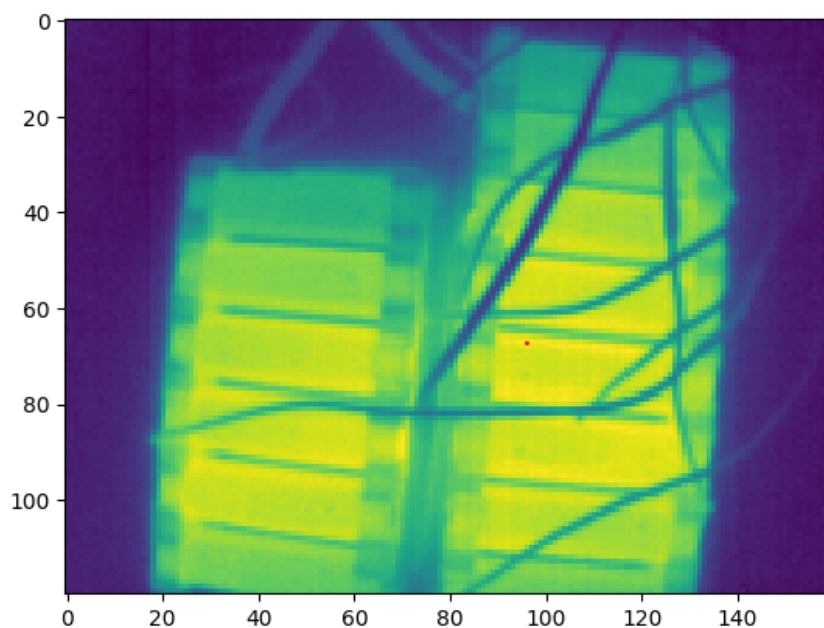


Figure 3.7: Example of a colorized image.

sentation is very intuitive and makes it immediate to understand the trend of temperature on the object, gathering many information on a single frame. For this reason, it is very useful for human understanding, thus ideal to show data and monitor the process progress in operation, but it is not suitable to be used as input to the control. As previously mentioned, temperature is the chosen control variable, with the aim of avoiding battery overheating while discharging at the highest possible speed. It is therefore sufficient to give as control input the maximum temperature on the pack for each moment, regardless of where it is located. To obtain it, a function searches for the maximum number of the camera's output matrix, that enters the control loop.

Another advantage of using a thermal camera consist of the possibility of visually locating where the hot-spots are within the battery, for each sample, and save these data obtaining their evolution along time.

In figure 3.7, that represents a battery pack thermal detection colorized with the technique explained above, also the maximum temperature point location is represented, identified by a small red dot on the image.

Analysis of hot-spots evolution over time may be interesting for further studies on batteries discharge.

3.7.1 Flat Field Correction

Flat-field correction (FFC) is a technique used to improve quality in digital imaging. It cancels the effects of image artifacts caused by variations in the pixel-to-pixel sensitivity of the detector and by distortions in the optical path [8].

In general terms, FFC is used to correct:

- Differences of light sensitivity between the pixel sensors of a camera.
- Differences of illumination intensities in the field-of-view.
- Differences in the transmission of light through the lens (for instance: vignetting).

The goal is to correct the pixels of the captured (raw) images in order to obtain an uniform resulting output when a uniform background is captured by the system (camera & lens). Once a detector has been appropriately flat-fielded, a uniform signal will create a uniform output (hence flat-field). This then means any further signal is due to the phenomenon being detected and not a systematic error.

In normal operating conditions, a detector (light sensor, vision system, camera, etc) is affected by distortion effects due to gains and dark currents.

In physics and in electronic engineering, dark current is the relatively small electric current that flows through photosensitive devices such as a light sensors (thus photodiodes) even when no photons enter the device. It consists of the charges generated in the detector when no outside radiation is entering the detector. It is referred to as reverse bias leakage current in non-optical devices and is present in all diodes. Physically, dark current is due to the random generation of electrons and holes within the depletion region of the device. Dark current is one of the main sources for noise in image sensors. The pattern of different dark currents can result in a fixed-pattern noise, which can be estimated. Nevertheless, the dark current itself has a shot noise (which can be represented as a Poisson random variable), which therefore results in a time variant noise.

The flat-field correction performed by FLIR 3.5 thermal camera consist on the compensation of offset errors described above, in order to obtain a more realistic thermal image, then a better temperature detection.

The correction consists on three main steps:

- Flat-field image acquisition
- Dark image acquisition
- Correction coefficients calculation

The first step in calibration consist on taking the flat-field capture. A flat-field image is acquired by imaging a uniformly "illuminated" surface, thus producing an image of uniform color and brightness across the frame. In thermal imaging this refers to the infrared radiation that hits the camera, it is thus needed a uniform temperature surface.

The second data required is the "Dark Image". Also known as dark frame, it is an image captured in the "dark", therefore in a condition where the camera sensor is not excited by

external radiation. Such image represents the dark current of the sensors, and is considered as a fixed bias that we want to eliminate when acquiring images in normal conditions. To acquire it, it's necessary to cover the lens and take a capture.

For the current application, FFC has to be taken "online", during operations. For this purpose, the camera is equipped with a moving shutter, able to cover the whole camera field of view. Shutter is used to take the dark image.

Once those images are available, correction can be computed. A flat-field consists of two numbers for each pixel, the pixel's gain and its dark current. The pixel's gain is how the amount of signal given by the detector varies as a function of the amount of light (or equivalent). The gain is almost always a linear variable, as such the gain is given simply as the ratio of the input and output signals. Dark-current has already been explained. To calculate the flat-field correction two values are computed [7]:

- Offset coefficients
- Gain coefficients

Offset coefficient is simply the dark current value detected for each pixel, through the dark image:

$$Offset_{row,column} = DarkImage_{row,column}$$

The offset correction matrix is obtained from combining these elements.

The gain calculation requires few more steps. First of all are defined the necessary terms, which description is reported in table 3.2 (capital letters are used for matrices).

C	corrected image	image obtained after FFC
R	raw capture	image acquired, not processed
F	flat-field image	uniform light pattern image
D	dark field image	uniform dark image
m	averaged value	target value for the pixels
G	pixels gain matrix	gain correction for pixels

Table 3.2: Flat Field Correction terms description.

Firstly, is calculated the target value that every pixel should have, basing on flat and dark images. The average on the flat image matrix gives the pixels goal value, on which the dark current correction is applied according to dark image matrix average value.

$$m = avg(F) - avg(D)$$

Each pixel should have this value. In order to achieve it, it's calculated the gain necessary for every element, according to the relation [7]:

$$m = (F_{row,col} - D_{row,col}) \cdot gain \tag{3.1}$$

Starting from relation 3.1 it is possible to obtain the gain for each pixel, rewritten in matrix form:

$$G = \frac{m}{F - D}$$

Knowing the gain for every pixel it is now possible to calculate the flat-field corrected

image:

$$C = (R - D) \cdot G$$

FLIR 3.5 thermal camera performs only one of the described corrections: offset compensation of the dark currents. In order to take the dark frame, shutter is closed, and a capture is taken, then used for the calculations.

Dark currents, in many detectors, such as thermal cameras, can also be a function of time. For this reason, it is necessary to continuously update dark currents value along operations. The default value of Lepton's flat-field correction time trigger is 180 seconds (3 minutes). When calibration occurs shutter closes and output data is frozen throughout the FFC event (nominally 0.4 sec) [8]. During and right after the calibration event, the output measure is heavily corrupted. As shown in figure 3.8, the correction leads periodically to high peaks on the measurement, with amplitude around 1.5 Celsius degrees, which distance the measure from its real value, and amplitude in terms of time of about 25 seconds. This effect is not negligible and may result problematic for some applications, it has to be treated.

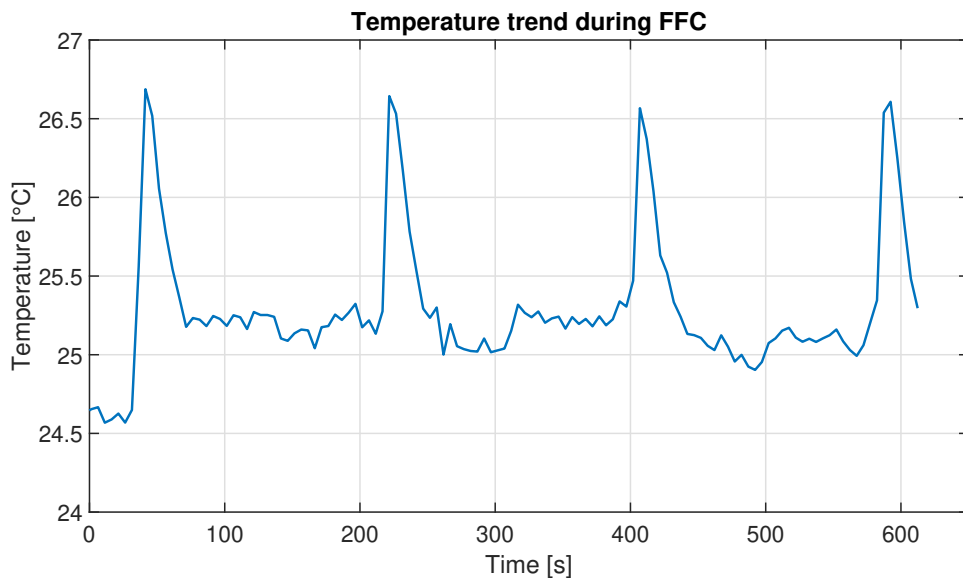


Figure 3.8: Temperature behaviour when Flat Field Correction occurs.

To cut the peaks due to the FCC, which only distort the measurement, there are two main possible solutions:

- Apply a low-pass filter
- Discard the distorted samples

Data filtering

Filtering data is the first solution usually considered when facing problems of noise or high frequency disturbances, but it may not always be the best solution. The main advantages and drawbacks will be considered below.

Generally, to clean a signal with a filter, it is necessary to know the disturbance and main signal frequency spectra. Knowing these parameters it is possible to set filter cut frequency in order to filter the disturbance and leave unchanged the signal of interest.

Low-pass filters are very effective, however, they introduce a significant delay on the system, directly proportional to filter capability to cut the noise. This is filters main drawback, and introduces a reduction in the overall system responsiveness.

In this case of study, the acting noise is known a priori. This gives an important advantage: the possibility of making the frequency analysis of the signal in order to determine noise dynamic and set the filter accordingly.

Another advantage introduced by the implementation of a filter is that all the eventual noise and high frequency disturbances acting on the system can be reduced, even if unknown or unexpected. It is indeed clear from the measure graph that, beside FFC, there are other phenomena that makes the measure very noisy, and this behaviour can be fixed thanks to the filter.

On this project, two types of filters have been tested in order to handle noise:

- **Butterworth filter:**

The Butterworth filter is a type of signal processing filter designed to have a frequency response that is as flat as possible in the passband, in order to approximate as much better an ideal filter. It is also referred to as a maximally flat magnitude filter.

To design a Butterworth filter some parameters has to be set, such as cut-off frequency, basing on the noise frequency; filter order (n), that determines frequency response amplitude slope after cut-off, equals to $n * (-20dB/dec)$;

The gain $G(\omega)$ of an n^{th} -order Butterworth low-pass filter is given in terms of the transfer function $H(s)$ as:

$$G^2(\omega) = |H(j\omega)|^2 = \frac{G_0^2}{1 + \left(\frac{j\omega}{j\omega_c}\right)^{2n}}$$

Where G_0 is the DC gain and ω_c is the cut-off frequency.

- **Finite Impulse Response (FIR):**

A Finite Impulse Response (FIR) filter is a filter whose impulse response (or response to any finite length input) is of finite duration, because it settles to zero in finite time. This is in contrast to infinite impulse response (IIR) filters, which may have internal feedback and may continue to respond indefinitely.

In case of an N^{th} order discrete time FIR filter, the impulse response (i.e. the output in response to a Kronecker delta input) lasts exactly $N+1$ samples (from first nonzero element through last nonzero element) before it then settles to zero.

For the filter design is used the "Windows design method". Which consist of a first design of an ideal IIR (infinite impulse response) filter and then truncating the infinite impulse response by multiplying it with a finite length window function. The result is a FIR filter whose frequency response is modified from that of the IIR filter.

Multiplying the infinite impulse by the window function in the time domain results in the frequency response of the IIR being convolved with the Fourier transform of the window function. If the window's main lobe is narrow, the composite frequency response remains close to that of the ideal IIR filter.

Samples digital selection

Another possible technique for dealing with the noise introduced by the FFC is to discard the FFC corrupted samples and replace them with a prediction based on past behaviour.

This kind of techniques are possible as it is used a digital control, which therefore allows samples manipulation.

The great advantage of this approach is that it doesn't introduce any type of delay, contrary to what happens when introducing a filter.

On the other side, during the time interval when samples are replaced with their predictions, input-output dynamic relation is temporarily lost, until real samples are acquired again. This is not a problem as long as the bound is lost for a period of time sufficiently short compared to the response time of the system.

For the purpose of this project, samples digital selection has been chosen. Both approaches was tested, but the advantage of not introducing any delay on the process produced better control results.

Chapter 4

Experimental Setup

In this section the experimental setup used for the project will be shown and explained. The various parts of the work required different equipment and tools, for this reason, two experimental setup has been used, both described below. The first setup was used to test the vision system and its operation for the analysis of the battery pack. A structured light camera was mounted on a robot arm that could move over the battery to take acquisition from different points of view. The robot was also equipped with an end effector that emulated the interaction of the arm with the battery pack.

The second setup was designed to test the final part of this project, the feedback control of the battery discharge. For safety reasons, the actual discharge tests were not carried out on the high voltage battery used for the vision tests, but on another battery pack, self-produced, of smaller size, to make it possible to treat it with the equipment available at the laboratory.

4.1 Vision system setup

The configuration used for testing the vision system consists of different elements, the main ones are listed below:

- ABB IRB 4400 robotic arm
- ABB IRBT X004 track motion
- ROS core
- Zivid one plus structured light camera
- Volkswagen Passat GTE Hybrid battery pack

4.1.1 Robotic arm

The manipulator engaged for this project is the ABB IRB 4400 (figure 4.1). This robot is an extremely fast and compact robot for medium to heavy handling. It has exceptional all-round capabilities which makes it suitable for a variety of manufacturing applications. On the 4400/60 version the load capacity of 60 kg at very high speeds usually permits handling of two parts at a time [1].

It is a 6-axis industrial robot, designed specifically for manufacturing industries that use flexible robot-based automation. The built-in process ware, has an open structure that is

specially adapted for flexible use, and can communicate extensively with external systems. The robot is equipped with the IRC5 controller and robot control software, RobotWare. RobotWare supports every aspect of the robot system, such as motion control, development and execution of application programs, communication etc [13]. The manipulator is available in two different versions: IRB 4400/60 and IRB 4400/L10. The difference consists on reach, respectively 1.96m and 2.53m, and handling capacity, respectively 60kg and 10kg. The 4400/L10 version has a longer final member, which ensures a wider working range (although reduced on the area closer to the robot and extended further away) but a lower payload, due to the increased torque resulting on the motors. For this project the IRB 4400/60 version is used.

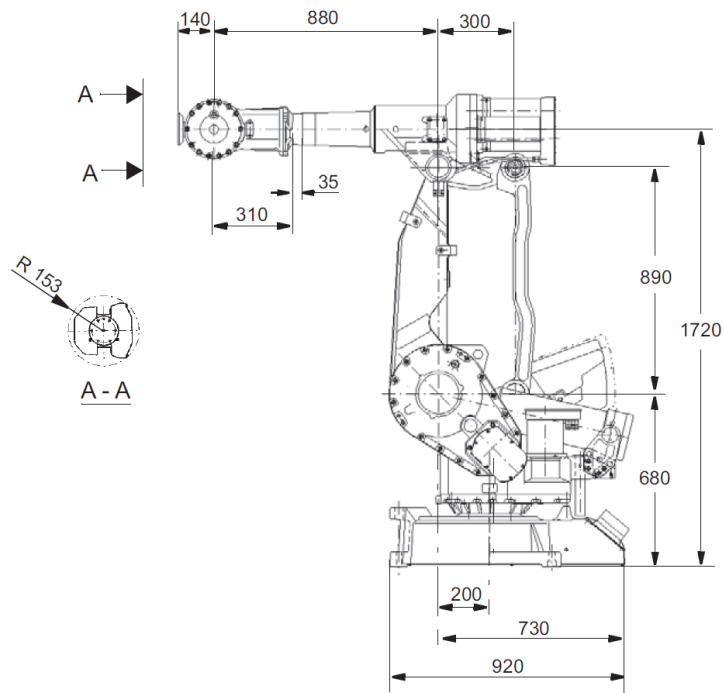


Figure 4.1: ABB IRB 4400/60 members dimensions

Its dimensions make it ideal to move around the battery pack and take acquisitions from different points of view, as well as allowing the robot to reach and act on every point of the battery pack as needed.

Manipulator main characteristics, according to data sheet [13], are tabulated below (table 4.1):

Variable	Value
Robot version	4400/60
Number of axis	6
Payload	60 kg
Reach	1.96 m
Position repeatability	0.06 mm
Path repeatability (1.6 m/s)	0.09 mm
Controller	IRC5

Table 4.1: ABB IRB 4400 technical data

4.1.2 Motion track

The robotic arm is not installed on the floor, but on a "moving platform" which acts as the 7th axis. This additional degree of freedom allows the robot to translate on a straight line along the Y axis. This feature can be useful for particularly large battery packs, in which the vision system is not able to acquire the whole pack with a single scan. In these cases, the track allows to move longitudinally along the battery pack, revealing the hidden part of the pack to the camera.

To be integrated with the IRB 4400 robot, the ABB IRBT 4004 was used (figure 4.2). It is an high class track motion from ABB, with company's unique Quick-Move and TrueMove, which can be fully exploited, that means optimal movement for the robot and the track with actual load, ensured by a seven-axis dynamic model. With compact, robust design and path accuracy and speed optimized, up to $2.0m/s$ and $2.5m/s^2$ acceleration [14].



Figure 4.2: ABB IRBT 4004 linear axis

4.1.3 Robot Operating System core

Robot Operating System (ROS or ros) is an open-source robotics middleware suite. Although ROS is not an operating system but a collection of software frameworks for robot software development, it provides services designed for a heterogeneous computer cluster such as hardware abstraction, low-level device control, implementation of commonly used functionality, message-passing between processes, and package management. Running sets of ROS-based processes are represented in a graph architecture where processing takes place in nodes that may receive, post and multiplex sensor data, control, state, planning, actuator, and other messages. Despite the importance of reactivity and low latency in robot control, ROS itself is not a real-time OS. It is possible, however, to integrate ROS with real-time code. Recently, ROS 2 has been released, with the aim of taking advantage of modern libraries and technologies for core ROS functionality and add support for real-time code and embedded hardware [6].

Software in the ROS Ecosystem can be separated into three groups:

- language-and platform-independent tools used for building and distributing ROS-based software
- ROS client library implementations such as roscpp (C++) and rospy (Python)
- packages containing application-related code which uses one or more ROS client libraries

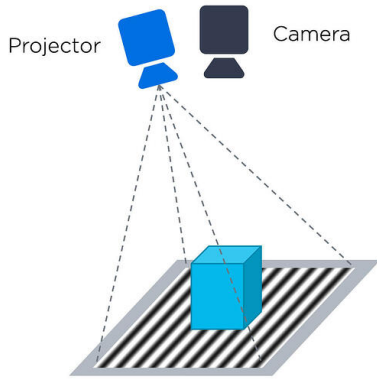


Figure 4.3: Zivid camera operation scheme.

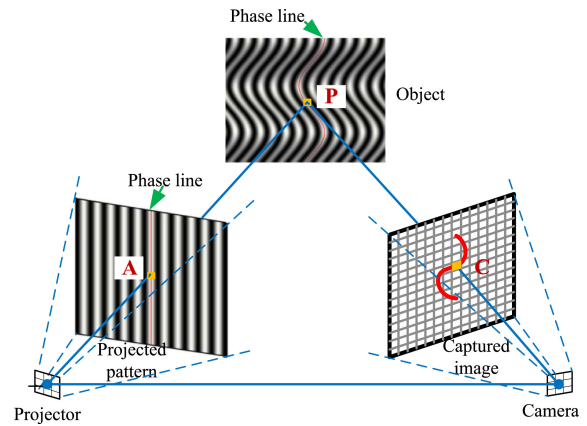


Figure 4.4: Light patterns projection, distortion and recognition on a structured light camera.

In this project, ROS is used to connect and communicate the different parts of the setup, explained above. In particular, ROS packages for the Zivid camera and IRB robot, permit to interface with the ROS core, hosted on the laboratory's computer. The "rospy" library, available for Python, gives the possibility to develop code to synchronize the different parts and act the task planning.

4.1.4 Zivid structured light camera

The central and most important part of the whole setup is the vision system. This has the task of identifying the battery connectors and determining their position in space. The precision of the operations that must be carried out requires that the camera is able to scan with good resolution, obtaining an accurate points cloud and therefore a precise pose estimation.

To achieve this objective, a structured light camera was used, the "Zivid One plus", medium size model. A structured-light 3D scanner is a 3D scanning device for measuring the three-dimensional shape of an object using projected light patterns and a camera system. Projecting a narrow band of light onto a three-dimensionally shaped surface produces a line of illumination that appears distorted from other perspectives than that of the projector, and can be used for geometric reconstruction of the surface shape.

A faster and more versatile method is the projection of patterns consisting of many stripes at once, or of arbitrary fringes, as this allows for the acquisition of a multitude of samples simultaneously. Seen from different viewpoints, the pattern appears geometrically distorted due to the surface shape of the object.

Although many other variants of structured light projection are possible, patterns of parallel stripes are widely used. The picture shows the geometrical deformation of a single stripe projected onto a simple 3D surface. The displacement of the stripes allows for an exact retrieval of the 3D coordinates of any details on the object's surface [31][32].

It's crucial to have an high camera resolution in order to obtain good pose estimation. Lower detection error leads lower positioning errors. Zivid is a state of the art camera and is able to take high resolution pictures, acquiring (1920 x 1200) size frames. It is

therefore possible to acquire a point cloud containing 2.3 million points (thanks to the 2.3 MP camera resolution).

4.1.5 Battery pack

The battery pack under test for this project is from the plug-in hybrid Volkswagen Passat GTE (figure 4.5).

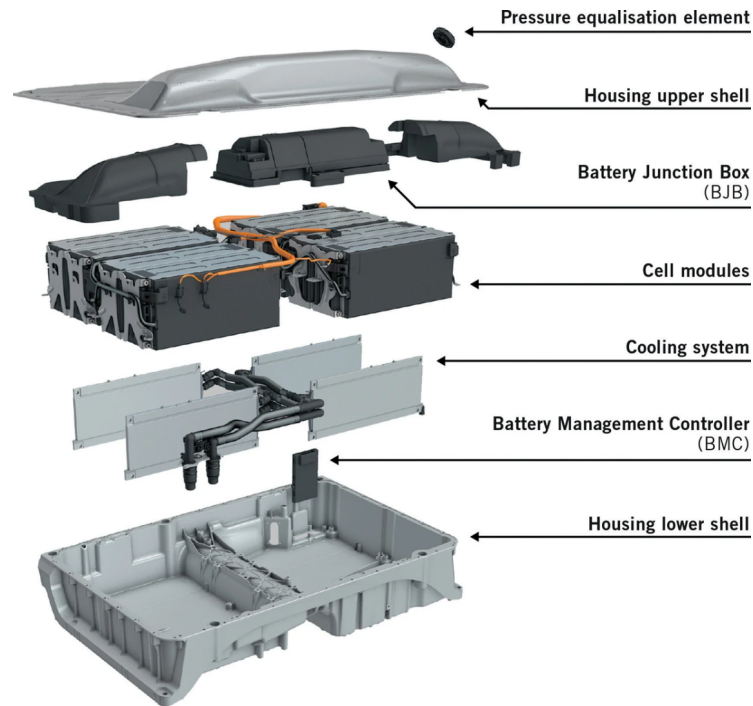


Figure 4.5: Volkswagen Passat GTE battery pack

The electrochemical energy storage system used for this vehicle is a modular lithium-ion high-voltage battery, designed for fully electric and hybrid operation of a plug-in hybrid vehicle. It consists of 96 prismatic cells with a capacity of 25 Ah each. Divided into four modules of twenty four cells each, this results in a rated energy content of 9.9 kWh at a rated voltage of 352 V.

The housing for the high-voltage battery consists of an upper section made from sheet aluminium and a lower section made from cast aluminium. Alongside the cell modules, the high-voltage battery also incorporates the battery management controller (BMC) and the battery junction box (BJB) containing the switching and measurement elements for the battery's high-voltage part [16].

Battery main specifications are reported in table 4.2.

4.2 Battery discharge setup

The second experimental setup is necessary to achieve the final part of the project, which consists of testing a possible methodology to discharge the battery pack. At this point, once previous parts of the project have been completed, the connectors of the battery pack have been identified and connected to the discharge device, it's now necessary to act the electrical discharge. As later explained in the "theory on discharge EV battery packs" chapter of this report, there are many possible industrial ways to discharge a battery,

Passat GTE battery pack	
Nominal energy	9.9 [kWh]
Usable energy	8.7 [kWh]
Modules	4
Cells per module	24
Total cells	96
Cells type	prismatic
Voltage	353 [V]
Nominal capacity	25 [Ah]

Table 4.2: Volkswagen Passat GTE battery pack specifications.

with their pros and cons. On this project, resistive discharge is proposed, monitored by a thermal camera. Normally, is set a constant discharge current, maintained until the end of the discharge, nevertheless, the proposed solution, provides that in order to increase the performance of the system, instead of implementing an open-loop control, the temperature of the battery pack is fed back, acting as control variable of a closed-loop system. This allows for a variable c-rate, reducing discharge time, but still ensuring a safe discharge, thanks to the camera temperature monitoring.

Electric vehicle's batteries work at high voltages, around 350 Volts, for this reason, conducting experimental discharge techniques might be dangerous, and requires specific and expensive instrumentation. For this reasons, as a first approach, it is better to start with a small battery pack, test the proposed process, and then, in case everything is correctly working, make further studies on bigger packs.

On this project, a small self-made battery pack is tested (figure 4.6). The main functions of the setup are to lead, control and monitor charge and discharge. Indeed, in order to carry out many experiments, after every discharge it is necessary to charge again the pack, to start a new cycle.

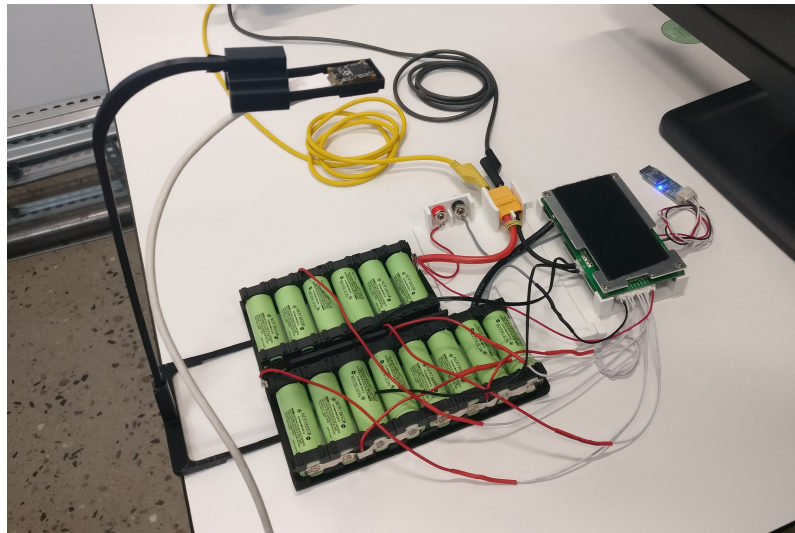


Figure 4.6: Battery discharge setup implementation.

Each test is divided into two phases: the charge phase, at the beginning, that leads to maximum state of charge the pack; and the discharge phase, the actual testing phase, with a variable c-rate controlled basing on the temperature detected by the camera. Different

components of the setup work on different phases.

The setup is composed by different devices and parts, the main ones are:

- Array 3721A programmable electronic load
- Array 3663A DC power supply
- 7 series of 2 parallel cells battery pack
- Battery management system (BMS 7S)
- FLIR PureThermal mini board & FLIR Lepton 3.5 thermal camera
- 3D printed mechanical support
- Central control unit (PC)

4.2.1 Programmable electronic load & DC power supply

The crucial part of the discharge system is the possibility of changing, as wanted, the discharge current. This feature is ensured by the programmable electronic load. A programmable load is a type of test equipment or instrument which emulates DC or AC resistance loads normally required to perform functional tests of batteries, power supplies or solar cells. By virtue of being programmable, tests like load regulation, battery discharge curve measurement and transient tests can be fully automated and load changes for these tests can be made without introducing switching transient that might change the measurement or operation of the power source under test [18].

In this project, during the second phase of each discharge test, a PID regulator determines the discharge current and communicate it to the load, that acts as actuator, changing the resistance of the circuit.



Figure 4.7: Setup instrumentation: Array DC power supply (left) and programmable load (right)

The DC power supply, instead, works on the first phase of the experiment, recharging the battery to prepare it to get discharged. Both equipment are from the Taiwanese "Array Electronic Company, Ltd", model 3721A for the load and 3663A for the DC supply. Main characteristics reported on table 4.3 [20][21].

Array 3721A - load		Array 3663A - power supply	
Max input voltage	80 V	Max output voltage	80 V
Max input current	40 A	Max output current	6.5 A
Max input power	400 W	Max output power	520 W
SCPI programming	supported	SCPI programming	supported
Battery discharge mode	available	CC-CV mode	available

Table 4.3: Array instruments technical specifications

Single cells		Battery pack	
Company	Panasonic	Number of cells	14
Model	NCR18650B	Series of	7 parallel pairs
Nominal voltage	3.6 V	Nominal voltage	25.2 V
Rated capacity	3350 mAh	Rated capacity	6700 mAh
Rated energy	12.06 Wh	Rated energy	168.84 Wh
Weight	48.5 g		
Energy density	676 Wh/l		

Table 4.4: Low voltage battery pack technical specifications

4.2.2 Low voltage battery pack & BMS

For reasons explained above, to test the control of the discharge it wasn't possible to use the EV battery pack, thus, a small low voltage battery pack, self-produced, has been made and used. This pack is composed of 14 cells, with 3.6V of rated voltage per each. The cells are parallel connected in pairs, forming 7 couples, which are in turn connected in series. The voltages of each pair add up for a total of 25.2V, which is the nominal voltage of the battery pack. Considering a rated capacity of 3350mAh for each cell [26], the battery pack results to have an overall capacity of 6700mAh. Table 4.4 reports cells main specifications, as reported in data-sheet [26].

The construction of the battery pack was completed with the addition of a Battery Management System (BMS). Although in the real case study the BMS is bypassed during the discharge, in the experimental setup a BMS is still necessary. This is because the presence of the BMS ensures that the battery pack is charged and discharged correctly, and that the maximum and minimum voltage values of the individual cells are not exceeded. This ensures that the cells are not damaged during the various tests, so that they can be charged and discharged several times, and therefore can be done more tests. The presence of the BMS does not alter the results of the experiment for the purposes of evaluating the methodology applied. The only difference is that in the real application, on the EV high voltage battery, without the BMS during discharge, the cells could be damaged, but this is not a problem as the cells have then to be recycled (the components are extracted) and not reused in other applications.

4.2.3 Thermal camera & mechanical support

The thermal camera has the purpose of monitoring the temperature trend on the whole battery pack, detecting any overheating and allowing the system to act accordingly. Positioning the camera at an appropriate distance (in our case around 20 cm) it is possible

to acquire the whole pack at once. The field of view (FOV) of the camera is divided into a matrix of 19200 pixels, for each of which the temperature relative to that area is given. This feature allows not only to determine which is the peak temperature of the battery pack, that is necessary for the control, but also to locate it on the battery pack, determining if there is an area that is more prone to overheating. This data are digitally transmitted via USB cable to the computer, which can easily elaborate it.

The chosen camera is the "Lepton 3.5" from "FLIR Systems". The FLIR Lepton is a radiometric-capable LWIR (Long-Wave InfraRed) OEM (Original Equipment Manufacturer) camera solution, very compact, and cheap compared to traditional IR cameras. Using focal plane arrays of 160x120 active pixels, Lepton could easily integrate into native mobile-devices and other electronics as an IR sensor or thermal imager. The radiometric Lepton captures accurate, calibrated, and non-contact temperature data in every pixel of each image [19]. Its small dimensions and high performance specifications, makes it the ideal camera for this project.

To complete the setup and assemble together in place the different parts, it was necessary to build a case for the cells and a support for the thermal camera. Being necessary for a specific application, both parts have been self-designed and self-produced from scratch, using a 3d printing process. As software for the design of mechanical parts was used "Autodesk Inventor 2021". The slicing process, hence converting the "solid" 3D model into a "printable layers" model and then into code readable by the 3D printer, was carried out by the slicer software "Ultimaker Cura v. 4.8". Lastly, "Ultimaker 2 Extended +" 3D printer was used to craft all the parts, using PLA+ plastic polymer as printing material.

4.2.4 Control unit & Operating logic

As just shown, this setup is composed of many different parts, which must work simultaneously and communicate. To coordinate and control the system, as central unit an "ASUS" PC is used. The advantage of having all USB interfaced components, makes it easy to connect to a normal PC. The core that manages the operations is a Python script, which, thanks to different libraries, can perform different tasks: handling the communication with the electronic load via SCPI (Standard Commands for Programmable Instruments) and with the thermal camera, regulating the temperature sampling frequency, acquiring images at fixed time intervals, highlighting the hot-spots localization, implementing a PID controller that regulates the current, estimating the remaining state of charge of the battery, showing in real-time via console the acquired data and saving them in CSV format.

Every single test is divided into two phases:

Phase 1: Charge phase

Phase-2: Discharge phase

The first one, it's just a preparatory procedure, that it's necessary to bring the battery to the same initial condition for each test, i.e. at the same state of charge (SOC) level, that is 100%, to make the test last as long as possible. The battery pack was built with only one external connector, to avoid the possibility of connecting at the same time both the supply and the load. For this reason, the first operation to perform consists of connecting DC supply cables to the battery connectors. Then, the BMS has to be unlocked (connecting via

Bluetooth), indeed, for safety reasons, in not operating conditions it opens circuit switches avoiding current circulation. At this point, it is possible to start the charging process, setting the parameters on the DC supply. Charging Lithium-Ion cells requires a particular operating mode, called CC-CV, that ensures cells to reach their full capacity, in a safe and long-life sustainable way.

CC stands for Constant Current, and it's a simple method that uses a small constant current to charge the battery during the whole charging process. CC charging stops when a predefined value is reached. This method is widely used for charging NiCd or NiMH batteries, as well as Li-ion batteries. The charging current rate is the most important factor, and it can significantly influence the battery's behavior. For this reason, the main challenge of CC charging is setting a suitable charging current value that will satisfy both charging time and capacity utilization. A high charging current provides a quick charge but also significantly affects the battery's aging process. A low charging current provides high capacity utilization but also produces a very slow charge, which is inconvenient, for instance, in EV applications.

On the other side, another method is CV charging, constant voltage, which regulates a predefined constant voltage to charge batteries. Its main advantage is that it circumvents overvoltages and irreversible side reactions, thus prolonging battery life. Since the voltage is constant, the charging current decreases as the battery charges. A high current value is required to provide a constant terminal voltage at a nearly stage of the charging process. A high charging current from 15 percent to 80 percent SOC provides fast charging, but the high current stresses the battery and can cause battery lattice collapse and pole breaking. The main challenge for CV charging is selecting a proper voltage value that will balance the charging speed, electrolyte decomposition, and capacity utilization. Generally, the CV charging method is efficient for speedy charging, but it damages the battery capacity. The negative effect is caused by an increased charging current at a low battery SOC (at the beginning of the charging process), where the current value is significantly higher than the nominal battery current. The high battery current causes the battery lattice frame to collapse and contributes to the pulverization of the active battery pole substance.

The CC-CV charging method is a hybrid approach that combines the two previously mentioned charging methods. It uses CC charging in the first charging stage, and when the voltage reaches the maximum safe threshold value, the charging process shifts to the CV charging method. The charging process is complete when the current levels off or when full battery capacity is reached. The charging time is mainly defined by the constant current value (CC mode), while the capacity utilization is predominantly influenced by the constant voltage value (CV mode) [29].

Once the maximum capacity is reached, second phase can start. The discharge phase is the real testing phase, since the objective of the experiment is to determine a discharge method. Firstly, has to be disconnected the DC supply, in favor to connecting the programmable load. Battery management system unlock is still necessary, in order to permit the discharge. The entire process is now controlled by the Python program, therefore no more actions are needed on the setup. The script gives the possibility to set different values, such as SOC final value (at which to stop the discharge), time limit, current saturation, disable or use PID controller, discharge current value (when PID is off) and more. When started, the program shows in real-time the information about the ongoing discharge, and

save them for further subsequent analysis. When the battery reaches its lower SOC level (or the threshold set on the script) the control unit stops the discharge.

At this point, one experimental cycle is concluded, and data are ready to be analysed. Going back to the phase one, it is possible to start a new experiment, changing, for example, PID tuning or other parameters.

Chapter 5

Results and Discussion

In this chapter are reported the results obtained with the experimental activity. The detailed explanation of how these have been carried out is given in chapter 3, while the description of the hardware and software experimental setup is given in chapter 4.

The discussion is divided into two sections, the first one for the computer vision part, and the second one for the discharge monitoring and control. On each section, the results obtained are shown and discussed.

5.1 Vision system

The vision system is the set of structured light camera, robotic arm and ROS core, which jointly perform the role of identifying the connectors of the battery pack, locating them in space and moving the system in order to make the connection.

The first goal of this project, is the training of YOLO, the vision algorithm, that has the role of performing object detection. With the resulting information, together with structured light camera's data, it is possible to localize connectors position within the 3D space.

The work reported on this section are the network training and detection results.

5.1.1 Training phase

Training images set is very important to be various and realistic. It's fundamental that it includes different pictures from possible working scenarios, in this way, once trained, the CNN will be more versatile, being able to adapt to different situations, even different from the training ones. For further theoretical details refer to section 3.3, "Training phase", at page 23 of this report.

For the neural network training, there are some main parameters that can be regulated, which leads to different resulting training, and thus detection performance, which are:

- Number of epochs
- Training set mix
- Network configuration
- Pre-trained weights

There are different available options for each parameter, the main ones that have been considered and tested are reported in table 5.1.

Parameter	Available or used options
Epochs	5
	50
	100
	200
	250
	300
Images set	different points of view different light conditions level of detail (relative distance)
Configuration files	yolov3.cfg yolov3-tiny.cfg yolov3-spp.cfg <i>modification of previous ones</i>
Pre-trained weights	yolov3.weights yolov3-spp.weights yolov3-spp-ultralytics.weights <i>previous training weights</i> <i>none - from scratch</i>

Table 5.1: Training parameters available options.

To find the best training configuration many have been tried, changing some of the parameters and noticing how they affect the detection results.

In order to evaluate how the training phase took place, some parameters are given as output from YOLO, these are both losses and evaluation metrics. The losses are computed on both training and validation set, in order to detect possible overtraining.

Among the various tests that have been carried out, one has been selected as the best configuration for this object detection task, which parameters are reported in table 5.2.

For the chosen configuration, all the training output parameters reach optimal values. The loss functions hit really low scores, and the evaluation metrics rise high close to the optimal value that is one. Table 5.3 reports the final values obtained with the given training.

For the training evaluation it is also important to evaluate the trend of these parameters, not just their final value. A decreasing trend along with epochs means that the network is still learning, but it is also important to monitor the fact that the network does not become too dependent on the data used for training.

Parameters configuration	
Epochs number	300
Configuration file	yolov3.cfg
Pre-trained weights	yolov3.weights
Training Images	overall pack images detailed BJB images

Table 5.2: Best training configuration parameters.

YOLO output parameters		YOLO evaluation metrics	
GIoU loss	0.149	Precision	0.942
Objectness loss	0.0549	Recall	0.977
Classification loss	0.0223	mAP(0.5)	0.975
		F1	0.959

Table 5.3: YOLO training output parameters and evaluation metrics.

Most of all, it is important to monitor the behaviour of the losses calculated on the validation set, because thanks to these it is possible to detect possible overtraining. As long as the losses have a monotonous decreasing trend, it means that no overtraining has occurred.

Figure 5.1 shows the trend of two evaluation metrics, the precision and the F1 score (which explanation is reported at section 3.3.3). Both values tend monotonically to one, and they settle to their final value around 200 epochs. The recall trend is not reported since its value grows fast immediately and settle around its final value within the first 50 epochs.

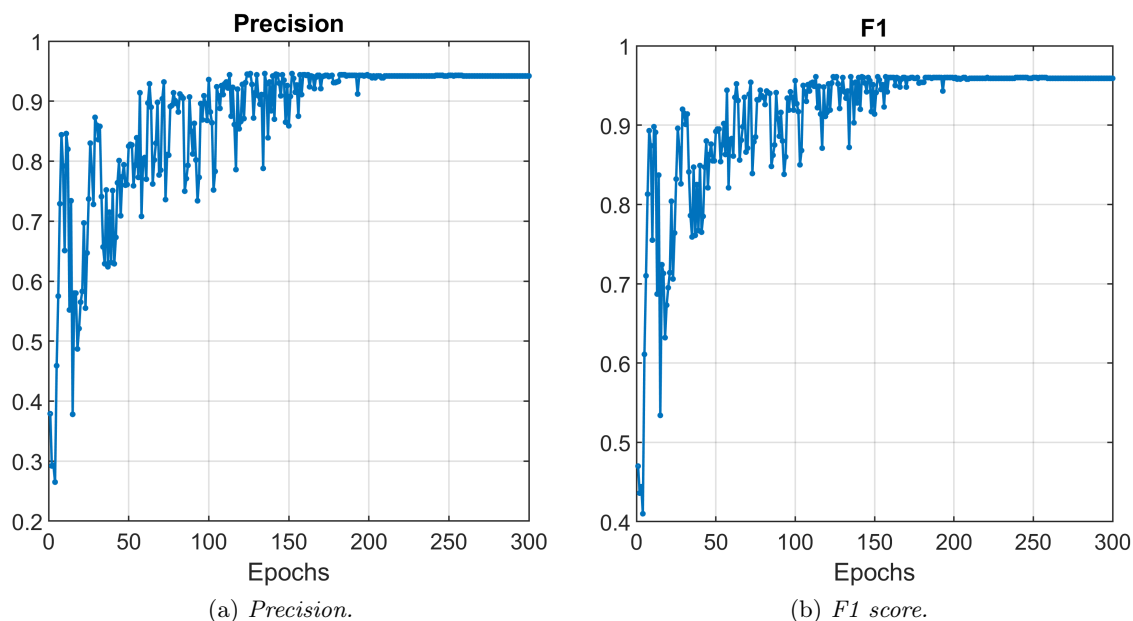


Figure 5.1: YOLO evaluation metrics: precision and F1 score.

Another important evaluation metric to consider, given as output from YOLO, is the mean average precision (mAP), which gives an overall view on training performances. Mean average precision is computed as the average of the AP value for different IoU threshold considered. Also this metrics shows an optimal result, settling on a value very close to one (figure 5.2).

In order to evaluate the training another important factor are the loss values, YOLO returns three values calculated both on the training set and on the validation set. Figure 5.3 shows the behaviour of the generalized intersection over union (GIoU) along the epochs, for both training and validation sets.

Another loss value given as output from YOLO that can be considered in order to evaluate the training performance is the objectness loss. Figure 5.4 reports the same comparison

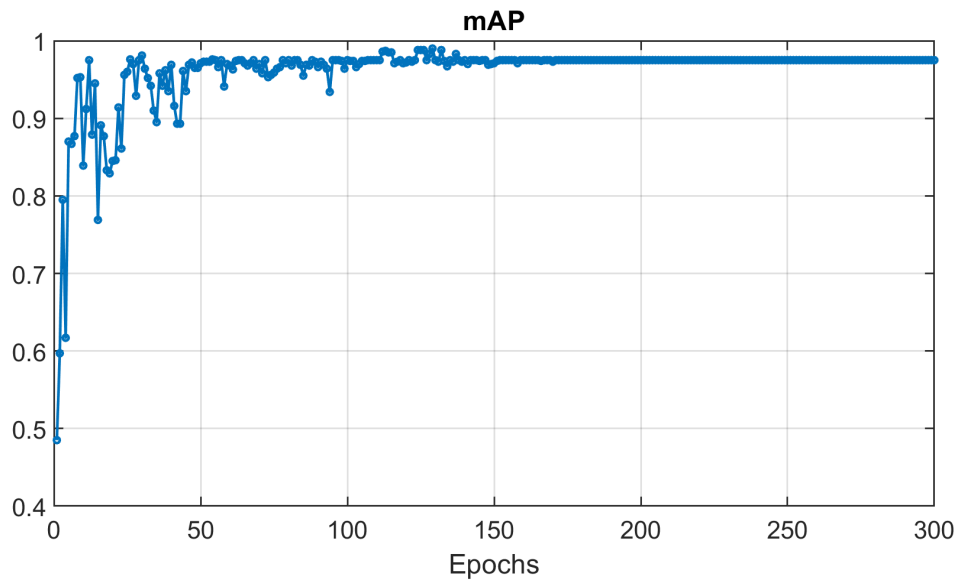


Figure 5.2: mean average precision evaluation metric.

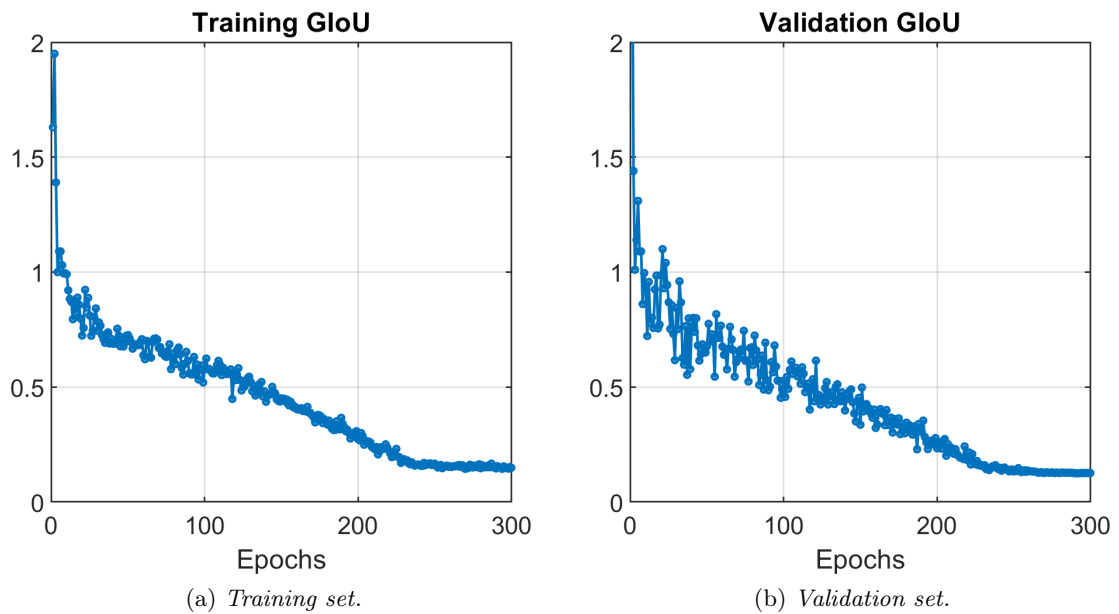


Figure 5.3: Generalized intersection over union loss computed for training and validation set.

Set	Overall	Detailed	Total	Percentage
Training	82	35	117	80%
Validation	20	9	29	20%

Table 5.4: Training and validation sets composition.

between training and validation set for the objectness loss.

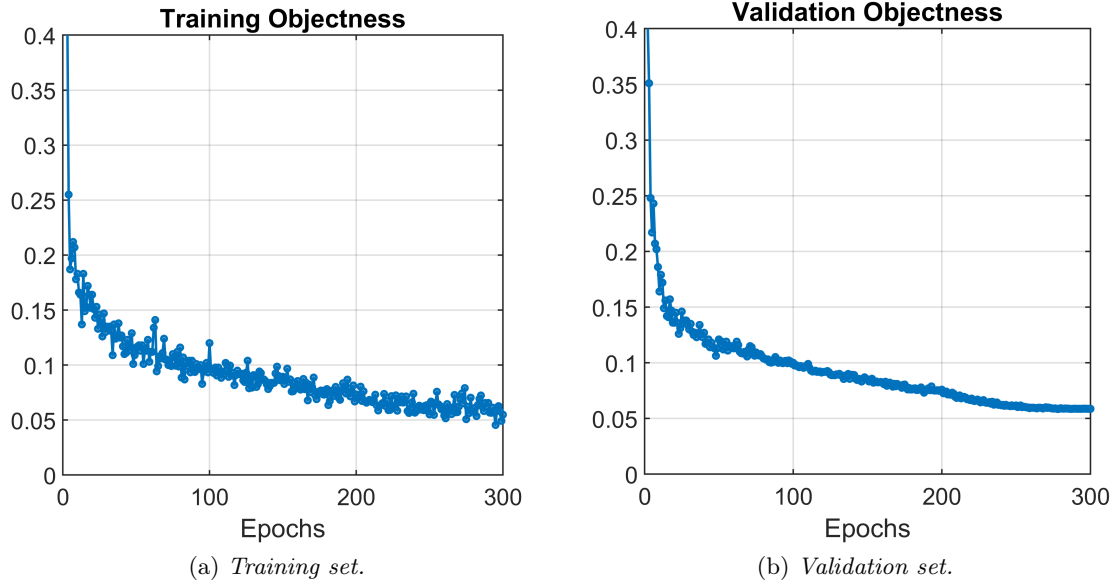


Figure 5.4: Objectness loss computed for training and validation set.

It's important to note that the loss value for both training and validation set is decreasing. This means that the system is not subject to overtraining. In case of overtraining, the loss calculated on the validation set would tend to increase at some point, because the network would lose its ability to generalize.

A total of 146 images were taken for the composition of the training and validation sets, all in the same working condition (for brightness). This is done to simulate a real operating situation, in which all images are taken in the same condition. Such images are all different, taken moving the camera in different points of view.

The training and validation sets composition is defined as follow (table 5.4). "Overall" refers to images of the whole battery pack while "detailed" refers to detailed images of the connectors, hence images taken closer to the battery junction box.

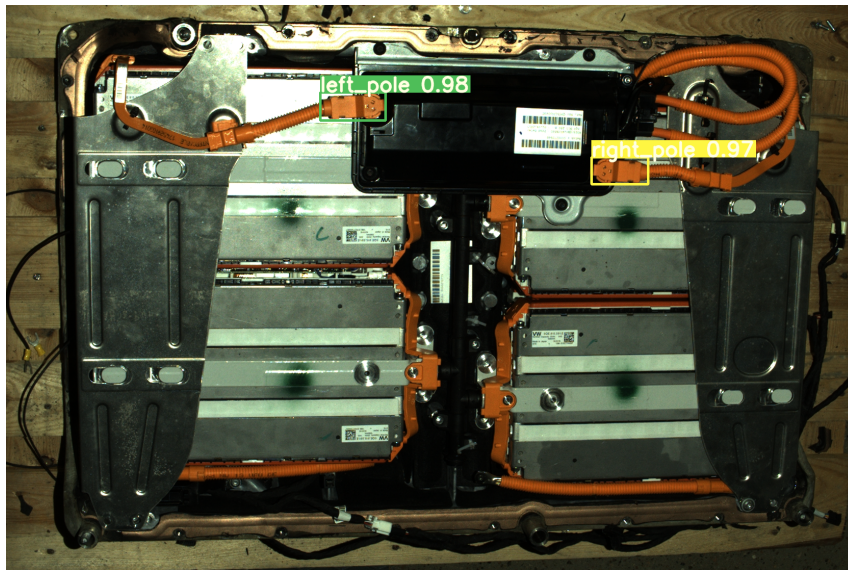
5.1.2 Detection phase

Once the network is trained it is possible to test the resulting weights on other images (inference phase), in order to evaluate system effectiveness and capability to generalize.

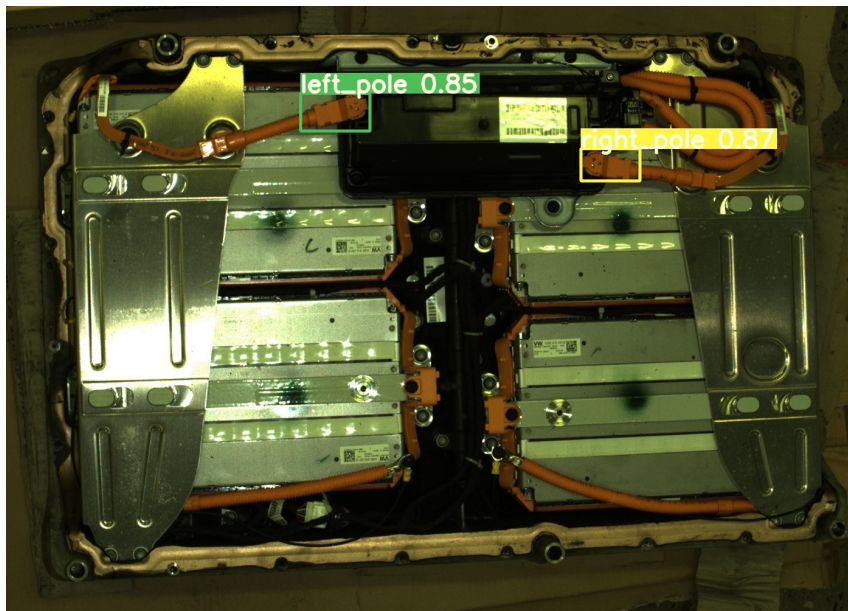
For this purpose, another images set is created, containing 40 images taken in different working conditions (many images is taken on each condition tested). Some of this images are reported below to show the detection results obtained.

The network proofed to be capable to adapt to different light conditions, correctly and precisely identifying the connectors. Figure 5.5 shows two different detection scenarios, with the laboratory illuminated by natural light (during day-time) and the laboratory illu-

minated with artificial light (during night-time). In both cases the localization is performed precisely, and the belonging class (left and right pole) are assigned correctly.



(a) *Natural light.*



(b) *Artificial light.*

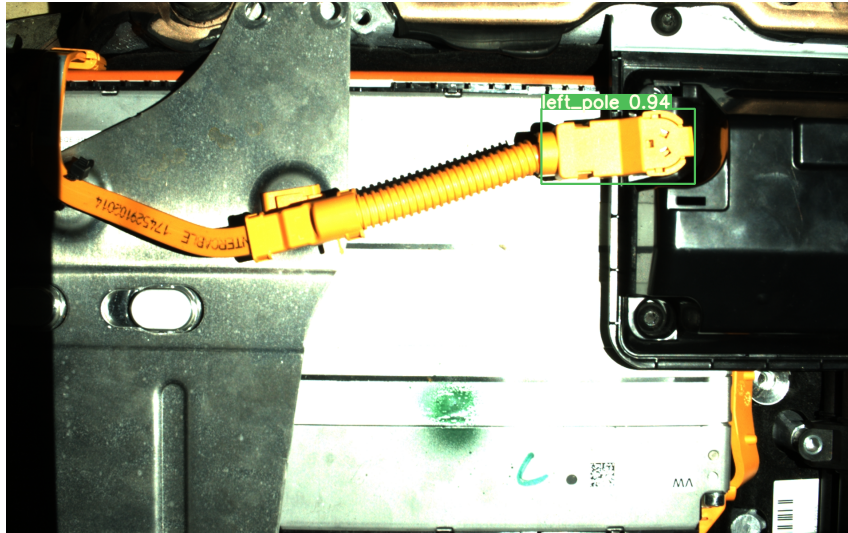
Figure 5.5: Detection with different light conditions.

The system is also capable of working from different camera-battery acquisition distances and different relative positions (different angles), therefore changing the point of view (POV). In figure 5.6 are reported two images taken from different POVs. Figure 5.6a is taken moving the camera very close to the left connector, and also presents a strong light reflection. Camera can also be moved in order to take pictures of the connectors from different angles, revealing a different view on the object, this is the case of figure 5.6b.

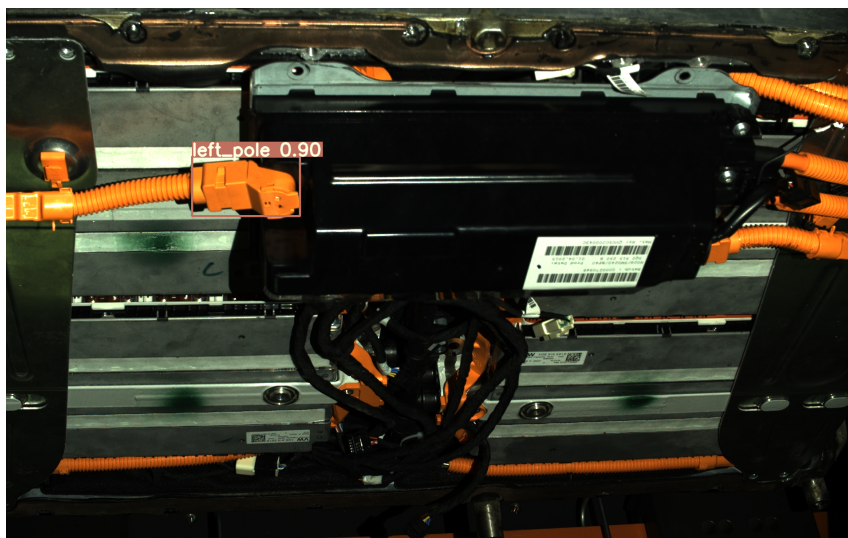
It is also interesting to note that the network correctly distinguishes and classifies the left and right connectors, even when only one of them appears in a picture.

The vision system has also demonstrated its operation, as well as for different lighting conditions, even in the case of very low lighting, this is the example shown in figure 5.7.

Pictures 5.7a and 5.7b are taken with two different settings for the structured light



(a) Close capture with presence of light reflection.

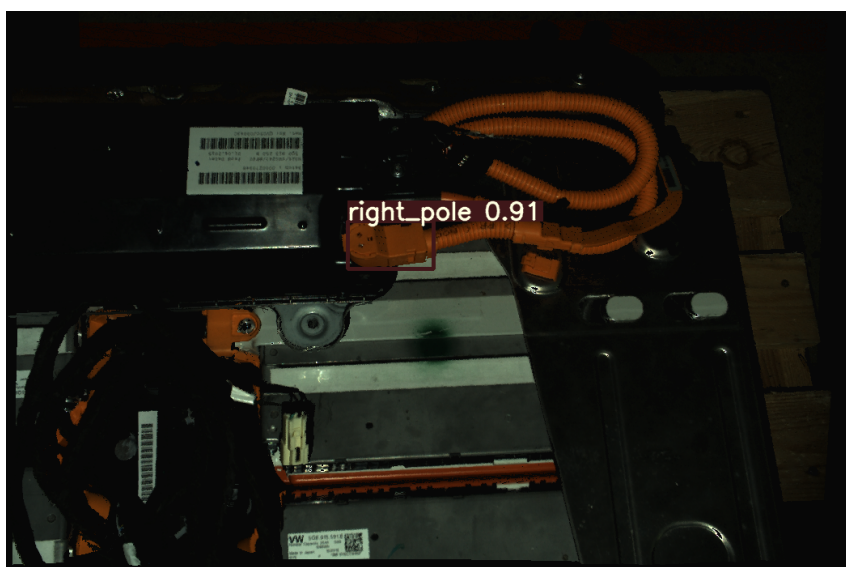


(b) View from other battery side.

Figure 5.6: Detection from different distances and points of view.



(a) *Reduced lighting.*



(b) *Very low lighting.*

Figure 5.7: Detection in reduced light conditions.

camera. Indeed, in order to obtain the best point cloud, there are some parameters that can be set, which are iris aperture, exposure time, stops value, projector brightness and sensor gain. Different configuration of such parameters may result in photo with different brightness, or, in general terms, these parameters are set for a specific lighting environment, and when the external conditions change, also the acquisition result different, and possibly very dark.

In the end, the last example reports a detection performed on a very critical situation, i.e. with the connector not fully visible but partially covered, because of the point of view the picture is taken from (figure 5.8).

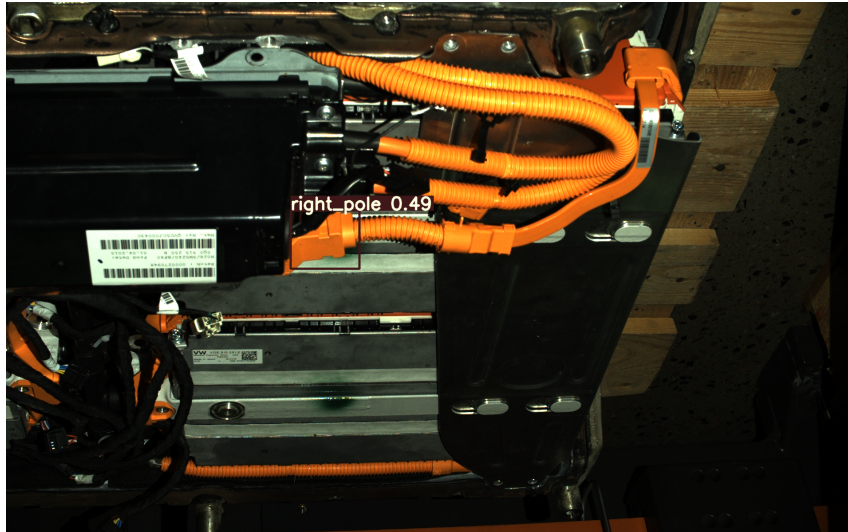


Figure 5.8: Detection with connector partially covered.

Even in such situation, the system surprisingly performs correctly the identification, both locating and classifying properly the connector.

This example further confirms the generalization capacity of the network, which has proved to be extremely flexible and versatile, capable of working in conditions significantly different from those used for training, and therefore of adapting to different work scenarios, a very important factor in future industrial use.

5.1.3 Pose estimation

Once the connectors are detected their spatial pose has to be estimated. The YOLO algorithm gives as output the coordinates of the predicted bounding box in terms of image pixels. The goal is to obtain the connectors position in the camera reference system.

In order to obtain these coordinates, a transformation must be applied from the coordinates in pixels to those in the real system (expressed in millimeters). To achieve it, it's necessary to know the Z coordinate of the connectors. The information is extrapolated from the depth image given as output from the structured light camera.

In this section will be reported an example for a single connector from a real case detection, to show how the pose estimation is carried out (the same procedure can be applied to both connectors identified). The same process has been repeated many times on different images, ad relative detections, in order to obtain a statistical sample of the accuracy of this system.

YOLO gives a prediction bounding box in pixels coordinates, showing the two left-down

x_1 [px]	y_1 [px]	x_2 [px]	y_2 [px]
783	242	902	170

Table 5.5: Predicted bounding box in pixels coordinates.

and right-up corners, as reported in table 5.5: From the bounding box corners it is possible to obtain the location of the pixel in the center of the box, corresponding to the connector location:

$$x_p = 842 \text{ [px]} \quad y_p = 206 \text{ [px]}$$

Thanks to this coordinates it is possible to obtain the z value of the pixel from the depth image (figure 5.9). The Z coordinate extracted is:

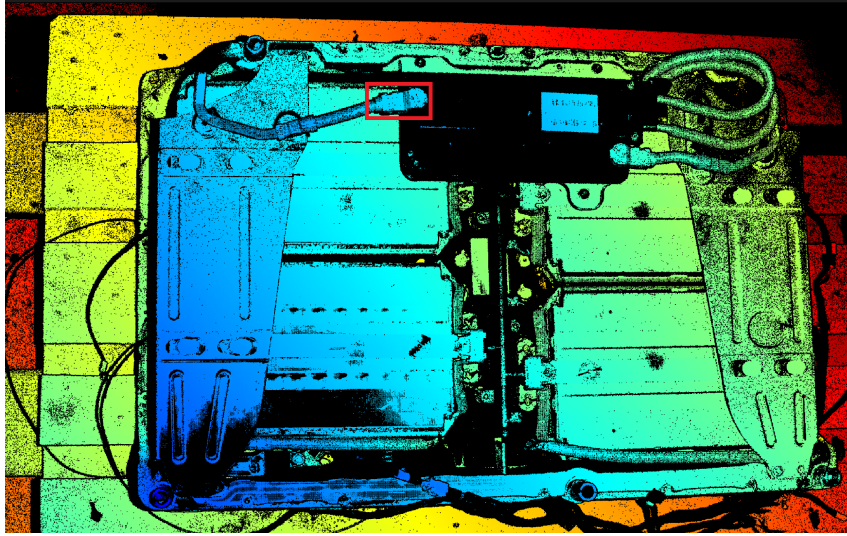


Figure 5.9: Depth image with YOLO predicted bounding box for z coordinate estimation.

$$Z = 1646.2 \text{ [mm]}$$

Thank to this data it is possible to calculate the X and Y coordinates of the central point of the connector in the camera reference system, starting from the pixel coordinates, obtaining the following estimated coordinates:

$$X_{est} = -62.4520 \text{ [mm]}$$

$$Y_{est} = -222.3881 \text{ [mm]}$$

In order to evaluate the accuracy of this estimation, it is compared with the position of the same location in the point cloud. Here, the position of each point is already in the camera reference system, it is therefore possible to make a comparison. The process of obtaining the point cloud coordinates knowing the pixel position is done manually, in order to compare this data with the one estimated automatically.

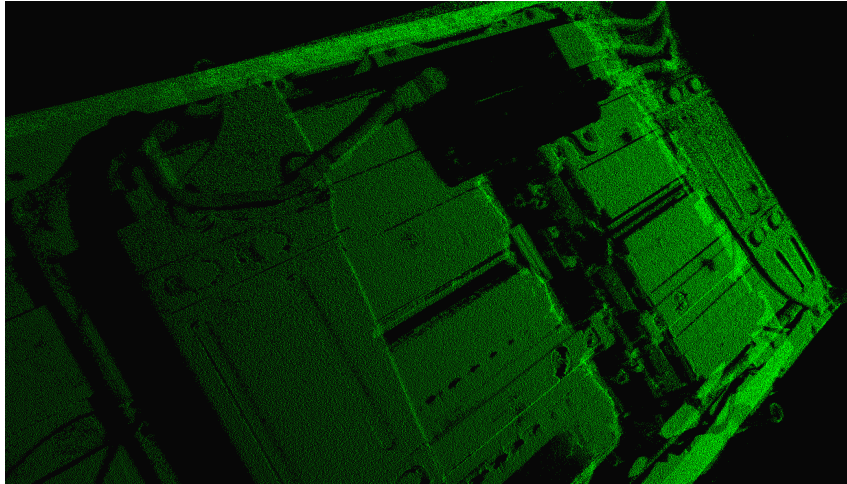


Figure 5.10: Point cloud (output of Zivid camera).

From the point cloud (figure 5.10) it results that the detected point coordinates are:

$$\begin{aligned} X &= -64.1 [mm] \\ Y &= -223.5 [mm] \\ Z &= 1646.2 [mm] \end{aligned}$$

The error compared with the estimation is really low, quantifiable in a few millimeters:

$$\begin{aligned} \Delta X &= X - X_{est} = -1.648 [mm] \\ \Delta Y &= Y - Y_{est} = -1.1119 [mm] \\ \Delta Z &= Z - Z_{est} = 0.00 [mm] \end{aligned}$$

According to this data, the estimation method proposed results to be very effective, guaranteeing an excellent position estimation in a completely automatic way, which also proved to be very accurate.

5.2 Discharge control

This are the results of the second, and final, part of this work. Once the first phase has been successfully completed, the system is electrically connected to the discharge device, and battery discharge can begin. The entire process is regulated by a closed loop control, as widely discussed in section 3.6, page 30 of this report. Basing on the data detected by a thermal camera that monitors the whole battery at once, the control loop decides the discharge current value, in order to always keep the temperature under a given limit. The chosen regulator is a PID controller, with proportional and integral actions, but not derivative (more properly known as PI controller).

On this section, are reported the results obtained implementing the discharge control previously discussed. In a first phase, the performance of the system without control will also be exposed, in order to make a comparison and therefore highlighting the increase in performance thanks to the proposed system.

All the experiments reported refer to the setup number two, as described in chapter 4 ("Experimental Setup"). The tests are indeed, for safety and hardware reasons, carried

Discharge parameters	
C-rate	0.5 C
Current	3.35 [A]
Target temp	-
Control	open loop
FFC correction	-

Table 5.6: Parameters settings for the open loop discharge.

out on a small battery pack, not on the high voltage EV pack used for the vision system tuning, which consists on the setup number one.

5.2.1 Open loop control

In order to make a comparison between the different discharge controls previously discussed, initially, the setup is used to test also some of the others techniques proposed, then showing the advantages introduced by the chosen control.

Open loop control is the currently used discharge method at "AS Batteriretur", partner of this project, and it is the process that wants to be improved, acting therefore as a benchmark for other discharge techniques.

In open loop control, there is no check on the reached temperature, for this reason, it's necessary to act with an important safety margin. Discharge current is set to a constant value, very low, in order to be sure that the pack never overheats, making temperature check unnecessary.

Referring to the available battery pack, a realistically low current may be equal to 0.5 *c-rate*. Having a rated capacity of 3220mAh for each cell [26], and considering battery pack electrical connections scheme, the discharge current is set to 3.35A . That is the output current of the whole pack, and it is numerically equal to 1C current for a single cell, however, cells are disposed in parallel in pairs, and therefore the total current is divided and each cell manages only half, corresponding to 0.5C for that cell.

Table 5.6 summarizes the setup parameters reported above.

Open loop control, as said before, for its definition doesn't require any check on ongoing temperature. However, the experimental setup prepared for the subsequent tests is used to monitor the temperature on the pack during the discharge, in order to evaluate this control technique. The detected temperature doesn't affect in any way the discharge, it is used for post-evaluation purposes only.

Figure 5.11 reports the experimental data acquired, showing how battery temperature evolves along the discharge test. On the plot are reported two Y-axes: the left one represents temperature in Celsius degrees, corresponding to the blue line; the right axis is instead the pack state of charge, which starts from 100% and decreases as the current flows, according to the red line. Time is reported on the X-axis, counting the minutes that elapse from the beginning of the discharge. The test lasted almost one and an half hour in total. The discharge, held with a constant current, discharged approximately the battery by 20%, bringing the state of charge from 100% to 80%.

It's evident from the graph that temperature follows a very "noisy" behaviour, with a lot of spikes repeated on a periodic basis. The reason is due to the technology used to detect the temperature, thermography. The thermal camera, indeed, every few minutes

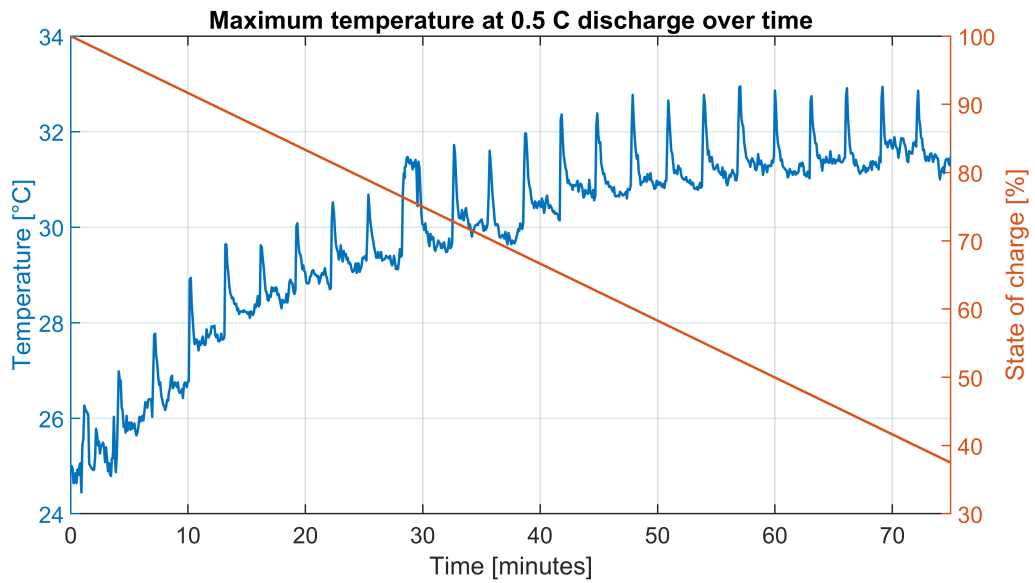


Figure 5.11: Maximum temperature on the battery and SOC over time for open loop control.

about acts a calibration in order to increase its accuracy, but this leads to the downside of generating this spikes every time, which are not related to the real temperature on the pack. Further explanation are reported at page 36 in subsection 3.7.1.

Neglecting these peaks, what matters most is the temperature trend. From the data, it is possible to make an interpolation and obtain the curve that represents its trend, which gives the information needed, reported in Figure 5.12. From the graph (Figure 5.12) it is

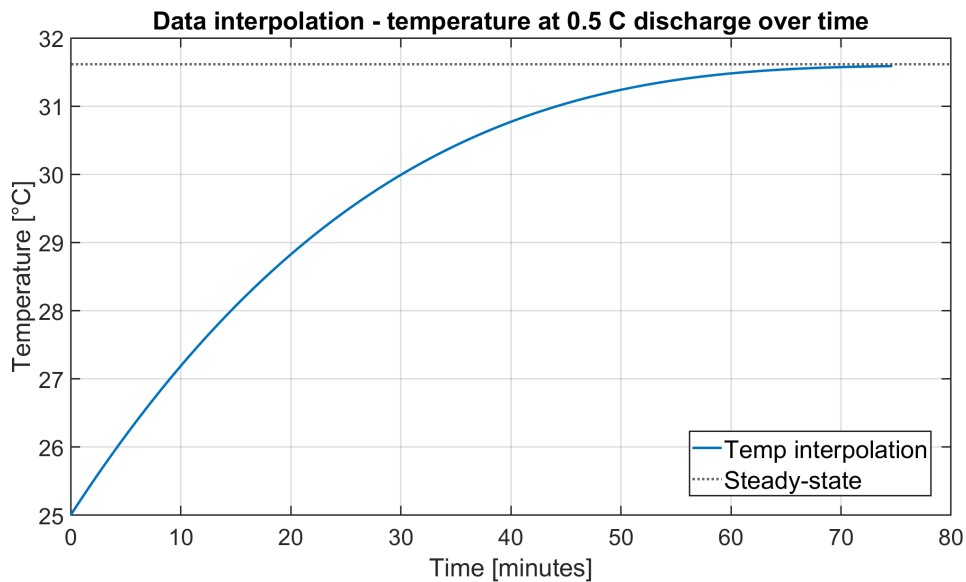


Figure 5.12: Temperature experimental data interpolation.

immediate to note that the one obtained is exactly the typical step response of a first order system, i.e. with the output quantity that immediately rises fast and then "slows down", tending asymptotically to the steady state value. Starting from the step response it is also calculated the time constant of the system τ , as the time needed to reach the 63% of the steady-state value:

$$\tau = 22.43 \text{ [min]}$$

the tangent to the curve at time 0, useful to obtain the time constant of the system.

During the 75 minutes of test, the system has reached its steady state temperature. For this reason, it is not necessary to continue the test in order to determine the final temperature, it will be the same being a first order system. On the other side, to determine the total discharge time (necessary to take the state of charge from 100% down to 0%), both the experimental approach, thus discharging all the capacity keeping track of the time needed, and the analytical approach, simply calculating mathematically the time needed knowing capacity and discharge current, can be used. Mixed approach is also feasible, discharging the battery of a certain percentage and then calculating the total time necessary for the remaining part.

From the test is also possible to derive the SOC evolution related to the discharge current, reported in figure 5.13.

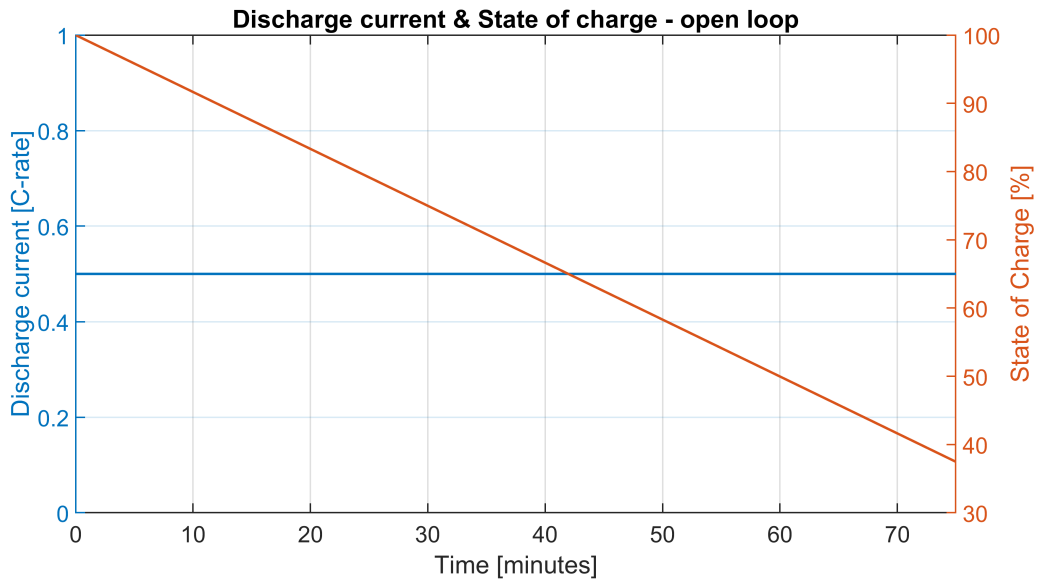


Figure 5.13: Discharge current and state of charge evolution over time for open loop control.

For this test, both behaviours are very simple: the current is kept constant for the whole discharge, and consequentially the SOC decreases linearly. This graph will be useful for making a comparison with the closed loop discharge, explained above.

The test reveals that the steady-state temperature of the system is around $31.5\text{ }^{\circ}\text{C}$, and the discharge time, for 60% SOC, is approximately 75 minutes. From the data obtained it is possible to extract the information regarding the full discharge with an open loop control, such as the time necessary for a full discharge and the maximum temperature reached. Table 5.9 summarizes these data.

Open loop - performance	
Full-discharge time (100% to 0%)	120 min
Steady-state temperature	31.58°C

Table 5.7: Open loop control - discharge output.

The open loop test reported in this section shows an important limit of the current setup, that hasn't been considered before: the large noise introduced on the detection by the thermal camera. For the purpose of this measurement, on this specific test, the

presence of noise does not involve any particular drawback. The aim was indeed to find the steady state value of the temperature for the open loop control, and thanks to the post-elaboration (thus not performed in real-time) it is possible to interpolate the data obtaining a "filtered" trend, not too influenced by the peaks, as wanted.

On the other side, it's a completely different matter with regards to feedback controls. In this case, the detected temperature is used as control variable, and therefore higher accuracy on the measurement leads to more precise control on the real pack temperature. Better measures are required.

The noise is introduced by an offset calibration process the camera performs periodically during operations, called Flat Field Correction (FFC). The calibration is aimed to improve image quality by compensating for certain offset errors that build up during camera operation. In order to do that, the shutter closes and acts as uniform temperature surface, allowing calibration.

In the subsequent tests, to prevent the alteration of measures, a digital "selection" of the samples has been performed, discarding calibration corrupted data. Further details on this phenomenon and possible solutions is reported at page 36 of this report.

5.2.2 Closed loop control with FFC correction

The closed loop control consists on a feedback control based on a PI controller. Compared to the open loop, explained above, the temperature is now monitored online and the discharge current is set accordingly to the error between target and detected temperatures.

Furthermore, has been introduced a "correction" for the noise introduced by the FFC, which is handled digitally, discarding the corrupted samples (more details at page 36).

In this case, to start the discharge, it is sufficient to set two parameters, and the rest is handled by the control:

- Maximum reachable temperature
- Maximum C-rate discharge value

The maximum temperature corresponds to the reference value that is given to the control, that is the value that must not be exceeded during the discharge. The c-rate, on the other hand, identifies the maximum current that the battery can withstand, and at the control level it corresponds to the maximum limit that is set at the output by the PI regulator.

These parameters have to be set basing on the maximum values that the battery can withstand under safe conditions. These can be estimated basing on battery nominal data or with laboratory tests. For the battery pack under test these were set as reported in table 5.8.

Discharge parameters	
Max C-rate	2 C
Max current	13.4 [A]
Reference temp	40 [°C]
Control	closed loop
FFC correction	digital

Table 5.8: Parameters settings for the closed loop discharge.

With these parameters the discharge test is performed. Figure 5.14 shows the closed loop system response. On figure are reported three data: the detected temperature; the interpolation polynomial and the temperature reference.

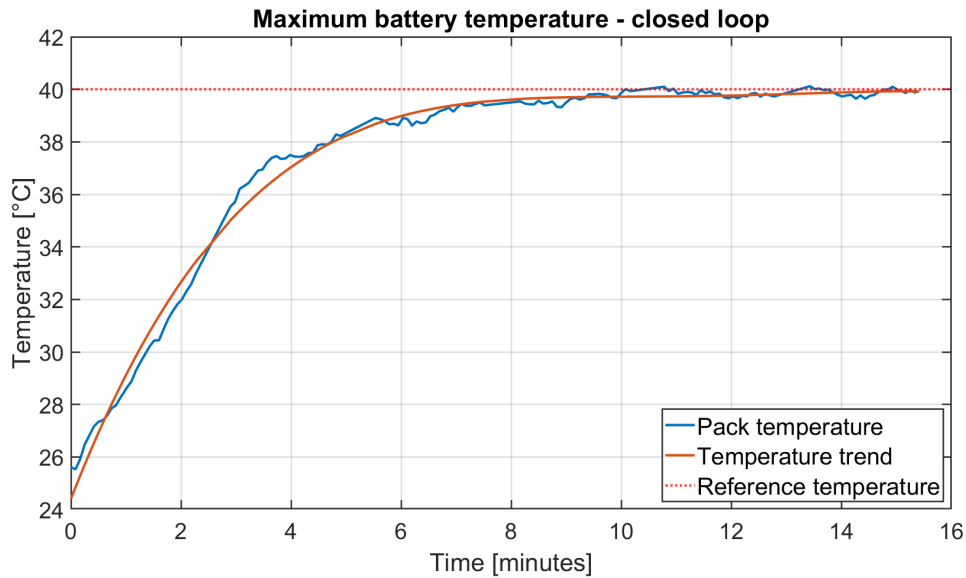


Figure 5.14: Maximum temperature on the battery over time for closed loop control.

Experimental data have a noisy behaviour due to the measurement, for this reason it is convenient to interpolate them in order to obtain a polynomial that fits their trend. The curve obtained can be used in the calculation of the time parameters of the response, such as rise time and steady-state error.

An important aspect to be noted is that the system has no overshoot. Considering this project application, it is crucial that the temperature doesn't exceed the maximum limit threshold set, involving safety issues.

In order to compare the closed loop control technique with the open loop, another important parameter to notice is the state of charge, and most of all its evolution over time. Being indeed the aim to perform the discharge as fast as possible, it's important to see how fast it decreases.

Figure 5.15 reports the battery SOC in percentage along the discharge, together with the discharge current, regulated by the controller, reported in terms of C-rate.

It's important to notice that, contrary to the open loop control (reported in figure 5.13), the discharge current it's not constant now, but varies according to battery temperature, because of the regulator. It is possible to interpolate the PID output in order to obtain its trend, shown in figure 5.16, which directly determines the discharge current.

Current variation has a great advantage, because the current directly determines the SOC slope: higher current leads to faster discharge. Such behaviour is evident in figure 5.15: in the first phase (from minute 0 to 3.5) the current is constant, leading to a SOC with linear trend and with maximum slope, being the time interval whereby the current has its maximum value. On the second phase (minute 3.5 to 12), current drops because of actual temperature reaching the maximum limit, and the SOC changes accordingly. The decrease is no longer linear, due to not constant current, and follows an "hyperbolic" trend. The third and final phase (12 to the end) registers a steady-state current that settles around a constant value, with some oscillation, leading again to a SOC with (approximately) a

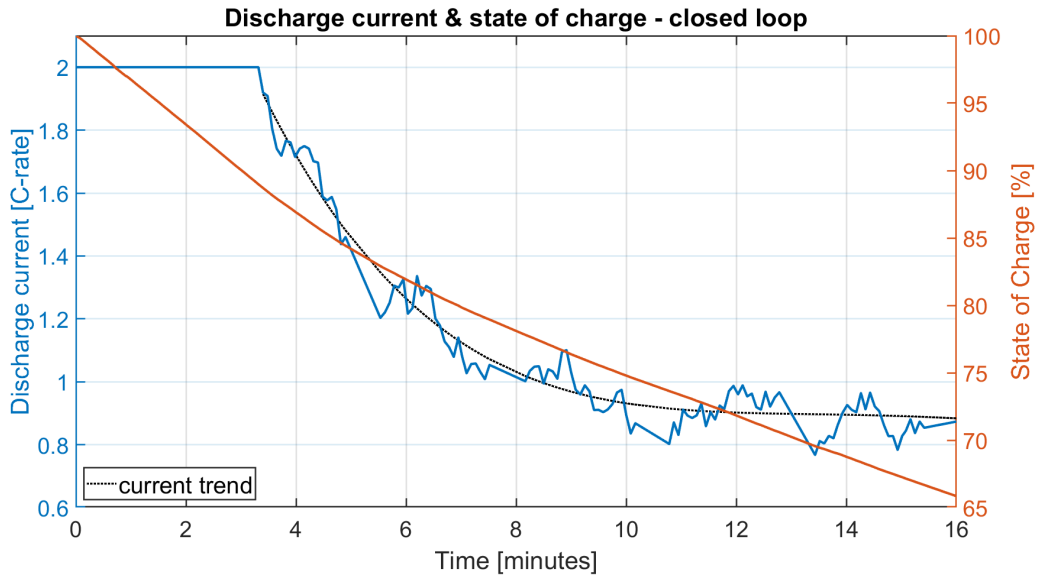


Figure 5.15: Discharge current and state of charge evolution over time for closed loop control.

linear trend. Which is the behaviour that will be kept until the end of the discharge.

Such data permits to determine total discharge time for the closed loop control case. Compared to open loop, system performance have increased significantly, leading to shorter overall discharge time.

Closed loop - performance	
Full-discharge time (100% to 0%)	58.8 [min]
Steady-state temperature	40 °C

Table 5.9: Closed loop control - discharge output.

It should be noted that, with respect to the previous case, even though the temperature reached at steady state is only slightly higher, the discharge times are instead considerably improved.

5.2.3 Results discussion

In the previous sections the results obtained by discharging the battery with the two different methods proposed were illustrated.

The experimental tests show, as expected, how the system dynamic is drastically improved thanks to the feedback control. The steady-state temperature is reached faster with the closed loop control, and this can be traced back to the fact that the current limit imposed on the system is greater.

In particular, open loop discharge is performed with a constant current of 0.5 C-rate, on the other side, closed loop maximum current is set to 2 C-rate, permitting system temperature to rise faster. Nevertheless, this current can't be kept for the whole discharge, in order to stay under the safety temperature limit.

The main objective of the control is to perform the discharge in the shortest possible time, given a temperature limit. In order to evaluate the discharge speed increase introduced by the system control, the comparison between three different tests is carried out.

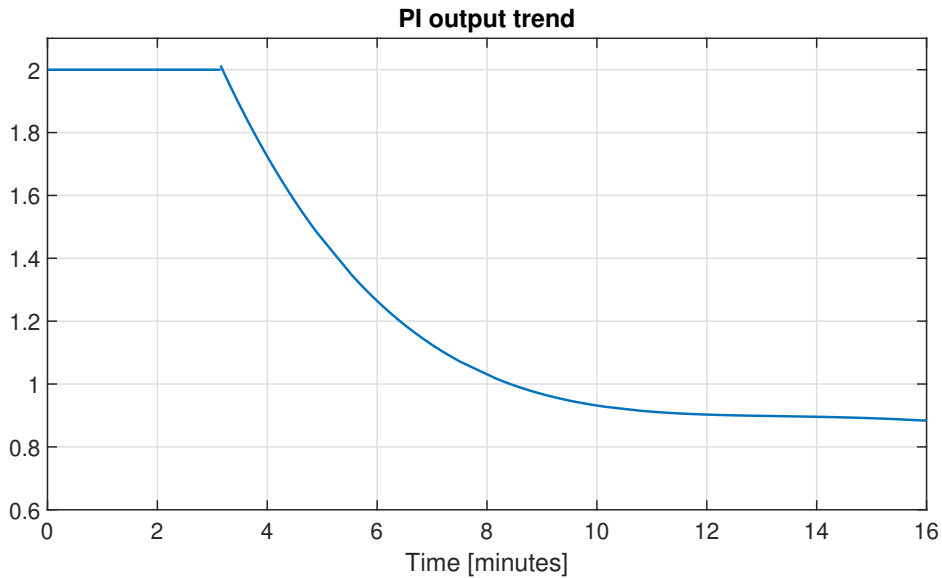


Figure 5.16: PID output trend.

The tests taken into account are described in table 5.10. Temperature refers to the steady-state temperature reached by the system. This value is imposed in closed loop control. Maximum current refers to the maximum limit set in closed loop control, for open loop, on the other side, refers to the constant current used for the discharge. Current value is expressed as discharge rate, with C as c-rate¹.

Test	Type	Temperature	Max current
1	open loop	31 [°C]	0.5 C
2	closed loop	40 [°C]	2 C
3	closed loop	45 [°C]	2 C

Table 5.10: Discharge tests parameters.

For each of the tests, the evolution of the state of charge in relation to time is reported in figure 5.17, in order to compare the different discharge times.

For test 1, discharge current is kept constant for the whole discharge, for this reason the state of charge decreases linearly without any change.

On the other side, test 2 and 3 has a variable current, this leads to a different variation of the SOC, that is linear in the first and in the final phases, when the current is constant. In between, there is a transient phase when current move from the initial value to the final one, changing the slope of the state of charge.

During the first phase, test 2 and 3 follow the same slope, both tests are indeed set with the same maximum current, that is used in the first phase.

The graph highlights the different discharge times required, significantly shorter for the closed loop than in the case of the open one, confirming the validity of the proposed system.

There is also a difference between different feedback control tests, thanks to the increase in the achievable temperature, in fact, the system can discharge with the maximum current for a longer time, and therefore discharge the battery more quickly, even with only 5°C of temperature difference.

¹C-rate is defined as the current that is necessary to discharge full capacity of a battery in one hour.

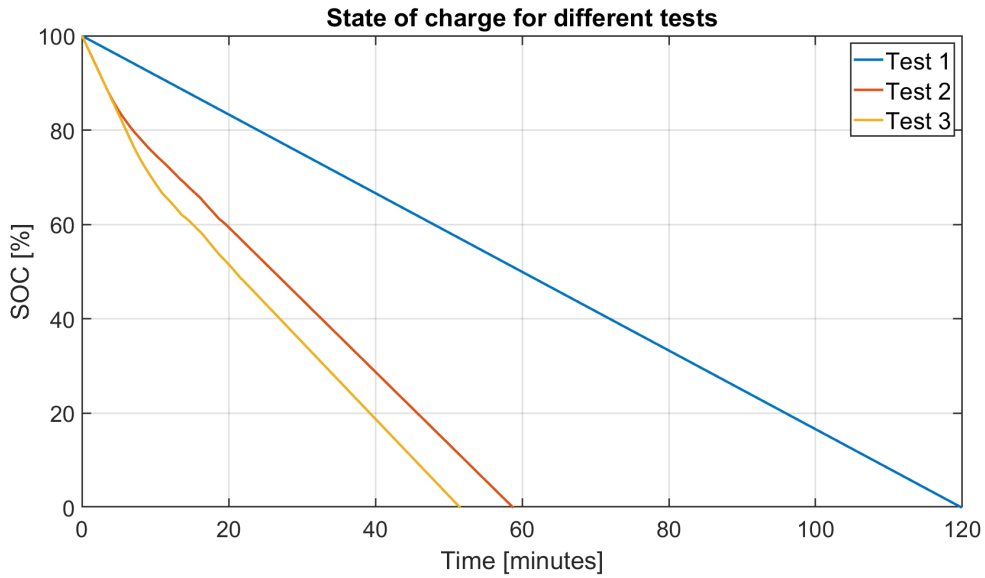


Figure 5.17: Discharge comparison between different tests.

Table 5.11 reports the discharge performance for different tests. Initial and final refers to the discharge current values in the initial and final part, therefore when the SOC variation is linear. Column " $\Delta\%$ " corresponds to the percentage variation of the discharge time with respect to the time taken as a reference, i.e. the time required for the open loop discharge (test 1).

Test	Initial	Final	Time	$\Delta\%$
1	0.5 C	0.5 C	120 [min]	-
2	2 C	0.8870 C	58.8 [min]	-51.0 %
3	2 C	1.0479 C	51.5 [min]	-57.08 %

Table 5.11: Discharge tests results.

It is important to notice that although both test 2 and 3 evolve with a linear trend in the final phase, they have different slopes, because of different discharge currents. This means that also in the final phase, higher reference temperatures are associated with faster discharges.

Chapter 6

Conclusions

This thesis project work aimed to develop the first steps in the design of an automatic discharging station for electric vehicle batteries, designing and testing the methodology that will be implemented on the final station. The objectives set at the beginning of the project have been successfully achieved.

The computer vision system has been implemented correctly and has shown to function under different operating regimes, upon different conditions.

The advantage of the proposed system consists in the possibility of training the neural network with a relatively small number of images (around a hundred) but still obtaining excellent identification results. This feature makes the system suitable for industrial applications, in which it is possible to train the system for a new battery pack in a short time.

The second part of this work consisted in the realization of an experimental setup for the discharge of a test battery pack. The temperature monitoring system was tested on this, using it to check the discharge current based on the detected temperature.

The proposed methodology, which envisages a thermal imaging camera in order to detect the maximum temperature reached by the battery pack, has proved to work very well for the problem to be treated, proving to be adequate for the necessary purposes and providing an excellent input to the control system.

On the other side, the control technique proposed, consisting of a PI regulator that follows a temperature reference setting the discharge current, proved to be effective and very responsive. The closed loop discharge control has significantly increased the discharge performance, considerably reducing the discharge time, compared to the open loop.

Experimental tests that have been performed show how, thanks to the feedback control, discharge time can be reduced up to almost 60%. On the test setup, on the same battery pack, discharging the full capacity without any feedback control requires 120 minutes, only 51 minutes are instead needed with closed loop control and 45 °C maximum temperature.

The result is obtained discharging with higher currents and reaching higher maximum temperatures compared to the open loop, condition made possible by the temperature detection.

Moreover, important safety improvements have been introduced on the system, because of the permanent battery maximum temperature monitoring, that ensures no overheating occurs in any phase of the discharge. Being overheating one of the main causes that may trigger battery fires and explosions during the discharge, due to internal chemical

phenomenon such as thermal runaway, a close real-time check on the temperature is a fundamental improvement.

The methodology proposed on this project for the design of an automatic electric vehicle batteries discharging station, proved to be effective and adequate to the objectives outlined at the beginning.

Further work is foreseen for this project, applying the same methodologies on different EV battery packs and prosecuting on the design of the automatic station through the design and test of the remaining station subsystems.

Appendix A

Discharge control Python scripts

This appendix chapter reports the self-developed Python code produced from scratch in order to realize the battery monitor and discharge setup (experimental setup number two).

A.1 main.py

```
import lepton_thermal_camera as camera
from lepton_thermal_camera.lepton_script2_v4 import *

import array_scp as array
from array_scp.SCPConfig import *

from functions import *
import os
from simple_pid import PID
from math import *
from scipy.signal import butter, filtfilt
from scipy import zeros, signal, random

# Default parameters - Array DC Load
termination_voltage = "17.5"
discharge_current = "0" # max = 5.9/6.4 A

# Real battery parameters
batt_capacity = 6.7 #[Ah]
rem_capacity = 6.7 #[Ah]
current_1c = 6.4 #[Ah] current at 1 c-rate

# Variables initialization - Thermal Camera
captures = []
last_FFC = time.time()
trigger_FFC = 0

# Default parameters - Total Test
test_time = 60*60*60 #[seconds]
time_interval = 5 #[second]
final_SOC = 35 [%]
```

```

SOC_start = 80 #[%]
snap_sampling = 5 #[seconds]
snap_history = []
timer = 0
phases = []

# PID tuning
Kp = 0.4
Ki = 0.0002810962754743500
Kd = 0
c_rate_lim = 2 #1.19
temp_goal = 45
pid = PID(Kp, Ki, Kd, setpoint=temp_goal)
pid.output_limits = (0, c_rate_lim)           # anti-windup
pid.sample_time = 0.01                       # Fixed optional update ...
        frequency of the PID

# Low Pass filter requirements (optional)
T = 40*60          # Sample Period (how long is the sampling test)
fs = 1/5          # sample rate, Hz
cutoff = 0.004    # desired cutoff frequency of the filter, Hz
nyq = 0.5 * fs   # Nyquist Frequency
order = 1        # sin wave can be approx represented as quadratic
n = int(T * fs)  # total number of samples

# FIR filter (uncomment to use)
# b = signal.firwin(order+1, cutoff) # FIR design based on wanted ...
        characteristics
# a = 1
# z = signal.lfilter_zi(b, a)        # construct initial ...
        conditions for the filter

# Butterworth filter (uncomment to use)
#normal_cutoff = cutoff / nyq
#b, a = butter(order, normal_cutoff, btype='low', analog=False) # ...
        butter filter
#z = signal.lfilter_zi(b, a)        # construct initial conditions ...
        for the filter (added by me)

# Log file managing - CSV
save_path = "data_log/"
date = datetime.now().strftime("%Y-%m-%d_%H-%M-%S")
csv_data_list = []
csv_heading_list = ["Time", "Termination ...
        Voltage", "Capacity", "Discharge Current", "Mean Temperature", "Max ...
        Temperature",
                    "Min Temperature", "State of Charge", "X max ...
                    location", "Y max location", "PID ...
                    out", "Filter Output"]
terminal_heading_list = ["\nTime", "Termination ...
        Voltage", "Capacity", "Discharge Current", "Avg Temp", "Max Temp",

```

```

        "Min Temp", "SOC", "X", "Y", "PID out", "Filter ...
        Out"]

# Captures saving
save_path_snap = save_path + ...
    "captures_saving/captures_{}/".format(date)
os.makedirs(save_path_snap)

# Hotspots saving
hotspots = numpy.zeros((120,160))

# Parameters settings - Array DC Load
battery_mode = array_load.query("BATT?")
if battery_mode != 1:
    array_load.write("BATT ON")

# -----
# MAIN:
# -----

# Cells position calibration
det_h = 120
det_w = 160
h_unit = det_h/8
w_unit = 20
pt_l=[]
pt_r=[]
w = []
cells = []
cells_matrix = numpy.zeros((120,160))
for c in range (8):
    pt_l.append( [ trunc(h_unit*(c+0.5)) , 90 ] )
    pt_r.append( [ trunc(h_unit*(c+0.5)), 90+w_unit] )
    w.append(trunc(h_unit/2))
    cells.append( Cell(pt_l[c],pt_r[c],w[c]) )
    cells_matrix [pt_l[c][0]] [pt_l[c][1]] = 1
    cells_matrix[pt_r[c][0]][pt_r[c][1]] = 1
for c1 in range(6):
    c = 8+c1
    pt_l.append( [ trunc(h_unit*(c1+2.5)) , 30 ] )
    pt_r.append( [ trunc(h_unit*(c1+2.5)), 30+w_unit] )
    w.append(trunc(h_unit/2))
    cells.append( Cell(pt_l[c],pt_r[c],w[c]) )
    cells_matrix [pt_l[c][0]] [pt_l[c][1]] = 1
    cells_matrix[pt_r[c][0]][pt_r[c][1]] = 1

# FUNCTION: recalibrate
ans = input("Show cell calibration (y/n)?")
if ans == "y":
    camera.lepton_script2_v4.numpyArr = None

```

```

calibration_capture = take_capture()
plt.imshow(calibration_capture)
plot_matrix(cells_matrix)
#plt.show()
plt.waitforbuttonpress()
while True:
    print("Stop the simulation now (ctrl+C).")
    time.sleep(1)

# User input - parameters initialization
print("PARAMETRS INPUT:")
rem_capacity = float(input("Insert the actual battery remaining ...
    capacity [Ah]: "))
SOC_start = rem_capacity / batt_capacity * 100
SOC_actual = SOC_start
test_time = int(input("Insert the safety time after which stopping ...
    the simulation [minutes]: ")) * 60

# User input - select modality
print("\nDISCHARGE MODALITY SELECTION:\n1) Normal 1 cycle ...
    discharge.\n2) Pulsed cycle discharge.\n")
mode, n_cycle = 1, "cyc0_" # delete data and use functions to normal use
if mode == 1:
    phases.append(Cycle(stop_SOC(SOC_start), 0))
if mode == 2:
    cycles_number = int(input("Insert the number of cycles: "))
    print("\n>> Cycles initialization: <<")
    for i in range(cycles_number):
        print("\n- Cycle {}".format(i))
        phases.append( Cycle( float(input("SOC discharge [%]: ...
            ")),int(input("rest time [minutes]: ")) ) )

# Data saving
with open(save_path + "log__" + date + ".csv", "w", newline="") as ...
    csvfile :
    logfile = csv.writer(csvfile, delimiter=',', quotechar='"', ...
        quoting=csv.QUOTE_MINIMAL)
    logfile.writerow(csv_heading_list)
    terminal_print(terminal_heading_list)

for phase in phases:

    #-- DISCHARGE CYCLE: --

    # Array DC load - settings
    array_load.write("BATT:CAP:CLE")
    array_load.write("BATT:TERM:VOLT {}".format(termination_voltage))
    array_load.write("BATT:CURR {}A".format(discharge_current))
    array_load.query("*OPC?")
    array_load.write("INP ON")
    array_load.query("*OPC?")

```

```

SOC_final = SOC_start - phase.SOC
end_time = time.time() + test_time
while (time.time() < end_time) and (SOC_actual > SOC_final):

    timer_sampling = time.time()

    # Array DC load query datas
    disch_time = str(array_load.query("BATT:TIME?"))
    disch_voltage = ...
        str(array_load.query_ascii_values("BATT:TERM:VOLT?")[0])
    disch_capacity = ...
        array_load.query_ascii_values("BATT:CAP?")[0]
    disch_current = ...
        str(array_load.query_ascii_values("BATT:CURR?")[0])

    # Lepton camera managing
    camera.lepton_script2_v4.numpyArr = None
    current_capture = take_capture()
    if current_capture is None :
        print("Error with current_capture occurred (thermal ...
            camera reboot needed).")
        save_hotspots(snap_history[-1].image, hotspots, ...
            save_path_snap)

    try:
        max_temp = centikelvin_to_celsius(current_capture.max())
        mean_temp = ...
            centikelvin_to_celsius(current_capture.mean())
        min_temp = centikelvin_to_celsius(current_capture.min())
        max_location_x, max_location_y = ...
            numpy.unravel_index(numpy.argmax(current_capture, ...
                axis=None), current_capture.shape)
    except:
        print("Error with current_capture (thermal camera ...
            reboot needed).")
        beeping()

    # Filtering (uncomment to use)
    # filter_out, z = filter_sbs(max_temp, z, b, a)
    filter_out = max_temp

    # PID update
    pid_out = pid(filter_out)
    discharge_current = pid_to_curr(pid_out, current_lc)
    array_load.write("BATT:CURR {}A".format(discharge_current))
    array_load.query("*OPC?")

    # SOC update
    SOC_actual = SOC_start - (disch_capacity / batt_capacity ...
        * 100)

```

```

# Cells update
for cell in cells:
    cell.update(current_capture)

# Data logging - CSV file
array_load.query("*OPC?")
data_list = [disch_time, disch_voltage, disch_capacity, ...
             disch_current, mean_temp, max_temp, min_temp, ...
             SOC_actual, max_location_x, max_location_y, ...
             pid_out, filter_out] # Add here variables ...
                                 name to print on csv file
csv_data_list = to_csv(data_list)
logfile.writerow(csv_data_list)
terminal_print(data_list)

# Captures logging
if (time.time()-timer)>=snap_sampling or True :
    snap_history.append(Snapshot(current_capture, disch_time))
    timer = time.time()
    snap_name = "capture__" + n_cycle + ...
               disch_time.replace(":", "-").rstrip() + ".png"
    plt.imshow(current_capture)
    plot_all_maxs(current_capture)
    plt.savefig(save_path_snap+snap_name, bbox_inches='tight')
    plt.close()

# Perform FFC
if (time.time()-last_FFC)>=(2.6*60):
    data_FFC = max_temp
    last_FFC = time.time()
    do_FFC()
    linear_prediction()
    trigger_FFC = 1

# Hotspot matrix save
hotspots[max_location_x][max_location_y] += 1

# Plot temp real time
count = count+1
if count >= 60:
    for image in snap_history:
        image.image.max()

frequency_check(timer_sampling, time_interval)

n_cycle = update_cyc(n_cycle)
SOC_start = SOC_actual

```



```

array_load.write("INP 0")

# --REST CYCLE:--
print("Rest cycle starts ({} minutes)...".format(phase.rest/60))
rest(phase.rest)

array_load.close()

# Print image hotspots
plt.imshow(snap_history[-1].image)
plot_matrix(hotspots)
plt.savefig(save_path_snap+"Hotspots_image",bbox_inches='tight')
plt.close()
plot_save_matrix(hotspots,save_path_snap)

# Save cells data
cells_header = []
row = []
for ind in range(14):
    cells_header.append("cell {}".format(ind+1))

N = cells[0].temp_story.length()
print("valore di N, lunghezza dati in Cell object:",N)

with open(save_path + "log__" + date + "_cells.csv", "w", ...
    newline="") as csvcells :
    cellfile = csv.writer(csvcells, delimiter=',', quotechar='"', ...
        quoting=csv.QUOTE_MINIMAL)
    cellfile.writerow(cells_header)
    for i in range(N):
        for c in cells:
            row.append(c.temp_story[i])
        csv_cell = to_csv(row)
        cellfile.writerow(csv_cell)
        row.clear()

# Errors checking
if len(data_list)!=len(csv_heading_list):
    print("WARNING! The number of elements on the CSV file doesn't ...
        match with the number of elements "
        "declared on the first row")

```

A.2 functions.py

```

from matplotlib import pyplot as plt
import time
import sys

```

```

import numpy as np
from lepton_thermal_camera.lepton_script2_v4 import *
from scipy import zeros, signal, random

def beeping():
    for n in range(5):
        print("\a")
        time.sleep(3)

def frequency_check (start,timer):
    # frequency regularization
    while (time.time()-start) < timer:
        time.sleep(0.01)

def to_csv(list):
    # convert the given list to be printed in csv file
    # -> convert in strings and remove newline characters
    output_list = []
    for data in list:
        data = str(data)
        output_list.append(data.rstrip())
    return output_list

def terminal_print (data_list):
    # print data on terminal
    string = ""
    for value in data_list:
        string = string + str(value).rstrip() + " | "
    string = string[:-3]
    print(string)

def modality_input ():
    # select input modality
    modality = int(input("Select the wanted discharge modality ...
        (1/2): "))
    n_cycle = ""
    if (modality != 1) and (modality != 2):
        print("Wrong input value. Please select value 1 or 2.")
        modality,n_cycle = modality_input()
    if modality==2:
        n_cycle = "cyc0_"
    return modality,n_cycle

def update_cyc (cycle):
    # update cycle number
    if cycle=="":
        return ""
    cycle = cycle[3:-1]
    number = int(cycle) + 1
    return "cyc" + str(number) + "_"

```

```

def plot_matrix (matrix):
    # plot the given matrix
    for row_n, row in enumerate(matrix):
        for col_n, element in enumerate(row):
            if element != 0:
                plt.plot(col_n, row_n, 'ro', markersize=1)

def plot_save_matrix (matrix, save_path):
    for row_n, row in enumerate(matrix):
        for col_n, element in enumerate(row):
            if element != 0:
                plt.plot(col_n, row_n, 'ro')    # tolto un - da qui ...
                                                in row_n
    plt.axis([0, matrix.shape[1], 0, matrix.shape[0]])    # tolto un ...
    - da qui in matrix.shape[0]
    plt.savefig(save_path+"Hotspot_matrix.png", ...
                bbox_inches='tight') #vedere come cambiare nome all'immagine
    plt.show()

def stop_SOC (start_SOC):
    end_SOC = float(input("Insert the SOC value that stops the ...
                          discharge: "))
    delta = start_SOC - end_SOC
    if end_SOC >= start_SOC:
        print("Wrong value! Final SOC has to be lower than starting ...
              SOC.")
        delta = stop_SOC(start_SOC)
    return delta

def save_hotspots (image, hotspots, save):
    # save hotspots location
    plt.imshow(image)
    plot_matrix(hotspots)
    plt.savefig(save + "Hotspots_image", bbox_inches='tight')
    plt.close()
    plot_save_matrix(hotspots, save)

def rest (seconds):
    # sleep cycle
    print("0%", end='')
    divisions = 100
    interval = seconds/divisions
    progress = ""
    for i in range(divisions):
        time.sleep(interval)
        perc = i + 1
        progress = progress + "|"
        sys.stdout.write('\r')
        print(progress + str(perc) + "%", end='')
    print("\n")

```

```

def pid_to_curr (controller, cr_1):
    return controller * cr_1

def plot_all_maxs (matrix):
    # plot all maximum values
    max_r,max_c = np.where(matrix == matrix.max())
    maxs_loc = list(zip(max_r, max_c))
    for max in maxs_loc:
        plt.plot(max[1], max[0], 'ro', markersize=1)

def LPF(data, cutoff, fs, order):
    normal_cutoff = cutoff / nyq
    # Get the filter coefficients
    b, a = butter(order, normal_cutoff, btype='low', analog=False)
    y = filtfilt(b, a, data)
    return y

def filter_sbs(data,z_prev,b,a):
    result, z = signal.lfilter(b, a, [data], zi=z_prev)
    return result, z

class Snapshot:
    def __init__(self,matrix,clock):
        self.image = matrix
        self.time = clock

class Cycle:
    def __init__(self,SOC,rest):
        self.SOC = SOC
        self.rest = rest*60

class Cell:
    def __init__(self,pt1,pt2,width):
        self.pt_left = pt1
        self.pt_right = pt2
        self.width = width
        self.sub_matrix = None
        self.temp_max = None
        self.temp_mean = None
        self.temp_story = []

    def update(self,matrix):
        rows = range ( self.pt_left[0]-round(self.width/2) , ...
            self.pt_right[0]+round(self.width/2) , 1 )
        columns = range ( self.pt_left[1] , self.pt_right[1] , 1 )
        self.sub_matrix = matrix[np.ix_(rows, columns)]
        self.temp_max = (self.sub_matrix.max() - 27315) / 100
        self.temp_mean = (self.sub_matrix.mean() - 27315) / 100
        self.temp_story.append(self.temp_max)

```

A.3 thermal_camera.py

```
from lepton_thermal_camera.import_clr import *

clr.AddReference("ManagedIR16Filters")

from Lepton import CCI
from IR16Filters import IR16Capture, NewIR16FrameEvent, ...
    NewBytesFrameEvent
from System.Drawing import ImageConverter
from System import Array, Byte
from matplotlib import pyplot as plt
import numpy
import time

def centikelvin_to_celsius(t):
    # conversion from centikelvin to celsius
    return (t - 27315) / 100

def to_fahrenheit(ck):
    # conversion to Fahrenheit
    c = centikelvin_to_celsius(ck)
    return c * 9 / 5 + 32

def getFrameRaw(arr, width, height):
    # frame callback function
    # this will be called everytime a new frame comes in from the ...
    # camera
    global numpyArr
    numpyArr = numpy.fromiter(arr, dtype="uint16").reshape(height, ...
        width)

def take_capture():
    capture = IR16Capture()
    capture.SetupGraphWithBytesCallback(NewBytesFrameEvent(getFrameRaw))
    capture.RunGraph()
    # wait until the capture operation is finished
    n = 0
    while (numpyArr is None): #and (n<=(20/0.1)) :
        n += 1
        time.sleep(.1)

        if n>=(15/0.1):
            initialize_lepton()
            return None
    capture.StopGraph()
    capture.Dispose()
    return numpyArr

def do_FFC ():
```

```

lep.sys.RunFFCNormalization()
time.sleep(30)

def colored_capture(matrix):
    # colourizing the matrix
    try:
        plt.imshow(matrix)
        plt.waitforbuttonpress()
    except:
        print("Exception on plotting image.")

def initialize_lepton():
    # lepton thermal camera initialization
    print("Problem! Stuck into the while loop waiting for a ...
          capture.") # initialize_lepton() #debug1
    for n in range(1):
        print("\a")
        time.sleep(1)

# INITIALIZATION:
# -----
lep, = (dev.Open() for dev in CCI.GetDevices()) #associate camera ...
      to lep

print("Camera connected with " + str(lep.sys.GetCameraUpTime()) + " ...
      uptime.")

```

A.4 import_clr.py

```

import clr
import sys
import os
import time

import platform

bits, name = platform.architecture()

if bits == "64bit":
    folder = ["x64"]
else:
    folder = ["x86"]

sys.path.append(os.path.join("../", *folder))
sys.path.append(os.path.join(*folder))
sys.path.append(os.path.join("lepton_thermal_camera", *folder)) # ...
      declare pkgs are in that folder

```

```
try:
    clr.AddReference("LeptonUVC")
except:
    print("\nError on finding the LeptonUVC.dll file:\n- Probably ...
        caused by changing the name of one of the folder of his path.")
    print("- Or because the file path location has ...
        changed.\nSOLUTION: Use original path/folders name or add ...
        the new path/names to os.path.join()\n\n")
```

Appendix B

Vision system Python scripts

On the current chapter are reported the Python utilities self-developed in order to ease the managing of training pictures and relative labels within the data-sets.

B.1 `paths_maker.py`

```
#script that create the .txt file containing the paths of all the ...
    images taht are used for the training

# HOW TO USE:
# - move this script "paths_maker.py" in the folder that contain ...
    all the training images and the labels
# - open the script and change the name of the variable ...
    'trainingFolder_name' with the name of the folder containing ...
    the training images that is on the side of the yolov3 folder*
# - open the teriminal in that folder and run the script (python3 ...
    paths_maker.py)
# - a file "paths_file.txt" will be created, containing the paths ...
    of all the images

# *note: to work properly yolov3 needs to have two different ...
    folders for the training images and for the yolo files, and ...
    they have to be side by side.
# This means that the structure of your directories has to be like ...
    this:
# >parental_folder:
#     >yolov3                               (containing yolo files)
#         >data
#         >cfg
#         ...
#     >trainingFolder_name                 (this is the folder on the ...
    side of the yolov3 folder. Put the name of this folder on the ...
    variable 'trainingFolder_name')
#     >training_img_test_1                 (this is the folder ...
    containing the training images. Put inside here this script but ...
    DON'T put this folder name in 'trainingFolder_name')
#         1.jpg
```



```

#             2.jpg
#             3.jpg
#             ...
#             >training_img_test_2
#             ...

import os

# path base
current_path = os.getcwd()
trainingFolder_name = "training_discharge" # name of the ...
# folder on the side of yolo folder
try:
    current_path.rindex(trainingFolder_name) # error ...
    checking
except:
    print("The folder containing the training images hasn't been ...
          found. Two probable casues:\n1) 'trainingFolder_name' ...
          inside the script paths_maker.py hasn't been changed (has ...
          to be the name of the folder containing the training images ...
          on the side of yolov3 folder) \n2) paths_maker.py scripts ...
          hasn't been moved to the folder containing the training ...
          images\n")
yoloFormat_folder = "../" + trainingFolder_name + ...
    current_path.split(trainingFolder_name,1)[1]
print("Folder containing training images path: " + ...
      yoloFormat_folder + "\n")

# read the .jpg .png files on a directory
supported_formats = ['.jpg', '.png']
files_names = os.listdir()

try:
    os.remove("paths_file.txt")
except:
    pass

paths_file = open("paths_file.txt", "a")

for file in files_names:
    for formats in supported_formats:
        if formats in file:
            paths_file.write(yoloFormat_folder + "/" + file + "\n")

paths_file.close()

print ("Operation completed successfully!! 'paths_file.txt' created.")

```

Bibliography

- [1] ABB. *IRB 4400 manipulator*. URL: <https://new.abb.com/products/robotics/industrial-robots/irb-4400>. (accessed: 15.03.2022).
- [2] Bonnie Baker. "Temperature sensing technologies." In: *AN679, Microchip Technology Inc* (1998).
- [3] Steinar Brandslet. *Researchers aim to recycle all the lithium in electric car batteries*. URL: <https://partner.sciencenorway.no/electric-cars-lithium-ion-batteries-ntnu/researchers-aim-to-recycle-all-the-lithium-in-electric-car-batteries/1605456>. (accessed: 13.05.2022).
- [4] Canalys. *Global electric vehicle sales up 109% in 2021*. URL: <https://www.canalys.com/newsroom/global-electric-vehicle-market-2021>. (accessed: 10.06.2022).
- [5] Atle Christiansen. *The University of Agder dismantles electric car batteries for reuse*. URL: <https://www.uia.no/en/news/the-university-of-agder-dismantles-electric-car-batteries-for-reuse#:~:text=Yes%5C%20please!-,The%5C%20University%5C%20of%5C%20Agder%5C%20dismantles%5C%20electric%5C%20car%5C%20batteries%5C%20for%5C%20reuse,of%5C%20recycling%5C%20electric%5C%20vehicle%5C%20batteries..> (accessed: 14.05.2022).
- [6] Amanda Dattalo. *Robot Operating System introduction*. URL: <http://wiki.ros.org/ROS/Introduction>. (accessed: 17.03.2022).
- [7] Euresys. *What is flat field correction?* URL: https://documentation.euresys.com/Products/Coaxlink/Coaxlink_10_3/Content/03_Using_Coaxlink/functional-guide/flat-field-correction/what-is-ffc.htm?TocPath=Using%5C%20Coaxlink%5C%7CFunctional%5C%20Guide%5C%7CAdvanced%5C%20Features%5C%7CFlat%5C%20Field%5C%20Correction%5C%7C_____1. (accessed: 15.04.2022).
- [8] *FLIR document number 102-PS242-40*. FLIR. URL: https://www.termocam.it/pdf/termocamere/flirtau2/tau2_spec.pdf.
- [9] Andreas Flórez. *Bombardier's PRIMOVE E-buses Pass 500,000 km Milestone*. URL: https://rail.bombardier.com/en/about-us/worldwide-presence/germany/en.html/bombardier/news/2017/bt_20170118_bombardiars-primove-e-buses-pass-500-000-km-mileston/en. (accessed: 26.03.2021).
- [10] Eric Gratz et al. "A closed loop process for recycling spent lithium ion batteries." In: *Journal of Power Sources* 262 (2014), pp. 255–262. ISSN: 0378-7753. DOI: <https://doi.org/10.1016/j.jpowsour.2014.03.126>. URL: <https://www.sciencedirect.com/science/article/pii/S0378775314004571>.

- [11] Kendrick Emma Harper Gavin Sommerville Roberto. “Recycling lithium-ion batteries from electric vehicles.” In: *Nature* (Nov. 2019). DOI: <https://doi.org/10.1038/s41586-019-1682-5>.
- [12] IEEE. *Technical committee for cognitive robotics*. URL: <https://www.ieee-ras.org/cognitive-robotics>. (accessed: 19.05.2022).
- [13] *IRB 4400-data sheet*. ABB. 2019-04-24. URL: <https://new.abb.com/products/robotics/industrial-robots/irb-4400>.
- [14] *IRBT X004-data sheet*. ABB. 2016-08-30. URL: <https://new.abb.com/products/it/3HEA802613-001/irbt-x004-track-motion>.
- [15] Roland Irle. *Global EV Sales for 2021*. URL: <https://www.ev-volumes.com/>. (accessed: 15.05.2022).
- [16] Pelz Norbert Jelden Hanno. “The Plug-in Hybrid Drive of the VW Passat GTE.” In: *MTZ worldwide* 76 (2015). ISSN: 2192-9114. DOI: <https://doi.org/10.1007/s38313-015-0038-2>.
- [17] Mark Potter Kate Abnett. *EU lawmakers back ban on new fossil-fuel cars from 2035*. 2022. URL: <https://www.reuters.com/business/autos-transportation/eu-lawmakers-support-effective-ban-new-fossil-fuel-cars-2035-2022-06-08/>. (accessed: 22.06.2022).
- [18] B.W. Leake. “A Programmable Load for Power and Noise Characterization.” In: *1982 IEEE MTT-S International Microwave Symposium Digest*. 1982, pp. 348–350. DOI: [10.1109/MWSYM.1982.1130715](https://doi.org/10.1109/MWSYM.1982.1130715).
- [19] Teledyne FLIR LLC. *LWIR Micro Thermal Camera Module - Lepton*. URL: <https://www.flir.co.uk/products/lepton/?model=3.5+Lepton&vertical=lwir&segment=oem>. (accessed: 06.04.2022).
- [20] Array Electronics Co Ltd. *DC loads - Array 372X series*. URL: <http://www.array.sh/yq-3721e.htm>. (accessed: 04.04.2022).
- [21] Array Electronics Co Ltd. *Switching power supply - Array 366X series*. URL: <http://www.array.sh/yq-366Xe.htm>. (accessed: 04.04.2022).
- [22] Alley R Manning P White E. “Vehicle System Design Process for a Series-Parallel Plug-in Hybrid Electric Vehicle.” In: *SAE International* (2012), pp. 503–524. ISSN: 2167-4191. DOI: <https://doi.org/10.4271/2012-01-1774>. URL: <https://www.sciencedirect.com/science/article/pii/S0956053X18301879>.
- [23] Nicole Nembhard. *Safe, Sustainable Discharge of Electric Vehicle Batteries as a Pre-treatment Step to Crushing in the Recycling Process*. Dec. 2019. URL: <http://hdl.handle.net/2117/334753>.
- [24] Severi Ojanen et al. “Challenging the concept of electrochemical discharge using salt solutions for lithium-ion batteries recycling.” In: *Waste Management* 76 (2018), pp. 242–249. ISSN: 0956-053X. DOI: <https://doi.org/10.1016/j.wasman.2018.03.045>. URL: <https://www.sciencedirect.com/science/article/pii/S0956053X18301879>.

- [25] Linda Olsson et al. “Circular Business Models for Extended EV Battery Life.” In: *Batteries* 4.4 (2018). ISSN: 2313-0105. DOI: [10.3390/batteries4040057](https://doi.org/10.3390/batteries4040057). URL: <https://www.mdpi.com/2313-0105/4/4/57>.
- [26] *Panasonic NCR18650B - data sheet*. Panasonic. URL: <https://www.batteryspace.com/prod-specs/NCR18650B.pdf>.
- [27] Hamid Rezatofighi et al. “Generalized Intersection over Union.” In: (June 2019).
- [28] Samveg Saxena et al. “Quantifying EV battery end-of-life through analysis of travel needs with vehicle powertrain models.” In: *Journal of Power Sources* 282 (2015), pp. 265–276. ISSN: 0378-7753. DOI: <https://doi.org/10.1016/j.jpowsour.2015.01.072>. URL: <https://www.sciencedirect.com/science/article/pii/S0378775315000841>.
- [29] Weixiang Shen, Thanh Tu Vo, and Ajay Kapoor. “Charging algorithms of lithium-ion batteries: An overview.” In: *2012 7th IEEE Conference on Industrial Electronics and Applications (ICIEA)*. 2012, pp. 1567–1572. DOI: [10.1109/ICIEA.2012.6360973](https://doi.org/10.1109/ICIEA.2012.6360973).
- [30] Kathrin Wegener et al. “Disassembly of Electric Vehicle Batteries Using the Example of the Audi Q5 Hybrid System.” In: *Procedia CIRP* 23 (2014). 5th CATS 2014 - CIRP Conference on Assembly Technologies and Systems, pp. 155–160. ISSN: 2212-8271. DOI: <https://doi.org/10.1016/j.procir.2014.10.098>. URL: <https://www.sciencedirect.com/science/article/pii/S221282711401155X>.
- [31] Song Zhang. “High-speed 3D shape measurement with structured light methods: A review.” In: *Optics and Lasers in Engineering* 106 (2018), pp. 119–131. ISSN: 0143-8166. DOI: <https://doi.org/10.1016/j.optlaseng.2018.02.017>. URL: <https://www.sciencedirect.com/science/article/pii/S0143816617313246>.
- [32] Zivid. *How it works - structured light*. URL: <https://www.zivid.com/3d-structured-light>. (accessed: 26.03.2022).